MARTIN MARIETTA ENERGY SYSTEMS LIBRARIES
3 4456 0153529 9

ORNL/TM-10302

ornl

OAK RIDGE
NATIONAL
LABORATORY

MARTIN MARIETTA

VELM61 and VELM22: Multigroup Cross-Section Libraries for Sodium-Cooled Reactor Shield Analysis

C. Y. Fu
D. T. Ingersoll

OAK RIDGE NATIONAL LABORATORY
CENTRAL RESEARCH LIBRARY
CIRCULATION SECTION
4500N ROOM 175
LIBRARY LOAN COPY
DO NOT TRANSFER TO ANOTHER PERSON
If you wish someone else to see this report, send in name with report and the library will arrange a loan.

OPERATED BY
MARTIN MARIETTA ENERGY SYSTEMS, INC.
FOR THE UNITED STATES
DEPARTMENT OF ENERGY

Printed in the United States of America. Available from
National Technical Information Service
U.S. Department of Commerce
5285 Port Royal Road, Springfield, Virginia 22161
NTIS price codes—Printed Copy: A04; Microfiche A01

This report was prepared as an account of work sponsored by an agency of the United States Government. Neither the United States Government nor any agency thereof, nor any of their employees, makes any warranty, express or implied, or assumes any legal liability or responsibility for the accuracy, completeness, or usefulness of any information, apparatus, product, or process disclosed, or represents that its use would not infringe privately owned rights. Reference herein to any specific commercial product, process, or service by trade name, trademark, manufacturer, or otherwise, does not necessarily constitute or imply its endorsement, recommendation, or favoring by the United States Government or any agency thereof. The views and opinions of authors expressed herein do not necessarily state or reflect those of the United States Government or any agency thereof.

ORNL/TM-10302
Distribution Category
UC-79-d

Engineering Physics and Mathematics Division

VELM61 AND VELM22: MULTIGROUP CROSS-SECTION LIBRARIES FOR SODIUM-COOLED REACTOR SHIELD ANALYSIS

C. Y. Fu
D. T. Ingersoll

Date Published: April 1987

Prepared for the
U.S. DOE Office of
Liquid Metal Converter Reactor

Prepared by the
OAK RIDGE NATIONAL LABORATORY
Oak Ridge, Tennessee 37831
operated by
Martin Marietta Energy Systems, Inc.
Under Contract No. DE-AC05-84OR21400
for the
U.S. Department of Energy

MARTIN MARIETTA ENERGY SYSTEMS LIBRARIES
3 4456 0153529 9

TABLE OF CONTENTS

ABSTRACT 1

I. INTRODUCTION 1

II. ANALYSIS OF THE SODIUM-IRON PROBLEM 3
- II.1 Computational Procedures 3
- II.2 The Reference 174n/38γ Calculation 6
- II.3 Group Structures 13
- II.4 Weighting Functions 15
- II.5 Additional Library Specifications 28
  - II.5.a Resonance Self-Shielding 28
  - II.5.b Temperature 29
  - II.5.c Legendre Order 30

III. CONTENTS OF THE LIBRARIES 32
- III.1 The Cross Section Libraries 32
- III.2 The Response Functions 36

IV. CONCLUSION 42

V. ACKNOWLEDGEMENTS 42

REFERENCES 42

VELM61 AND VELM22: MULTIGROUP CROSS-SECTION LIBRARIES FOR SODIUM-COOLED REACTOR SHIELD ANALYSIS

C. Y. Fu
D. T. Ingersoll

ABSTRACT

Two coupled neutron and photon multigroup cross-section libraries, derived from ENDF/B-V nuclear data, are described. The energy group structures, 61n/23γ and 22n/10γ, are subsets of the Vitamin-E 174n/38γ group structure, and are tailored to the iron and sodium resonances, windows, and capture gamma-ray spectra. Each of the two libraries are available in two formats, the AMPX master format and the ANISN format.

Cross sections for all materials in the Vitamin-E library were collapsed using a standard energy weighting function, and in addition, several cross-section sets for each of the major constituents of commercial grade sodium, stainless steel (types 304 and 316), and carbon steel were derived using several problem-dependent weighting functions for averaging the fine groups. Effects of various group structures and weighting functions on the accuracy of the broad group libraries are studied by ANISN analysis of a typical sodium-iron shield configuration.

I. INTRODUCTION

The generation of cross-section libraries with broad-group structures is primarily for economical reasons. It is not yet practical to perform two- and three-dimensional analyses using pointwise data or even fine-group cross sections such as contained in the 212-group Vitamin-E library.[1] Even for 1-D analyses, it is most efficient to begin a new shielding analysis with a few-group library and, as one understands the problem better, move to more accurate finer-group libraries. The establishment of reference broad-group libraries is desirable in order to avoid duplicated efforts among program participants and to assure a common data base used for design analyses. Additionally, validation of the

data via computational and experimental testing can be accomplished more efficiently.

Uncertainties are always introduced into the broad-group cross sections due to approximations in the weighting functions used for collapsing the fine groups. Intelligent choice of the weighting functions can reduce such uncertainties. Also, judicious selection of the energy group structure can help to reduce the dependence of the computed results on the weighting functions for a given class of problems. The selection of weighting functions and energy group structures is a central part of the present work.

The new broad-group cross-section libraries have been produced specifically for shielding analyses of liquid-metal cooled reactor systems. The names of the two libraries, VELM61 and VELM22, are acronyms for Vitamin-E Liquid Metal and the corresponding number of neutron groups. The libraries can be described as containing two parts. The first part includes all elements and isotopes in the Vitamin-E library (as of Aug. 20, 1985) and were collapsed using the standard weighting function given in Section II. The second part includes additional cross-section sets for the constituents of the mixtures used in a sodium-iron shield geometry analyzed as part of this study. These special cross sections were self-shielded at room temperature, and therefore, are composition-dependent. Entries for each major component in commercial grade sodium, type 304 stainless steel, type 316 stainless steel, and carbon steel are given for several different weighting functions. The latter includes the standard weighting function, the $1/E\Sigma_t$ (SS-304) and $1/E\Sigma_t$ (carbon steel) weighting functions, and several position-dependent fluxes calculated for a specific sodium-iron geometry.

Techniques for generating the new libraries and the effects of various group structures and weighting functions on calculated results for the sodium-iron problem are described in Section II. Also, effects of self-shielding, temperature, and Legendre order are presented. Section III gives the final library specifications and a description of a large variety of response functions. Section IV contains the conclusion.

II. ANALYSIS OF THE SODIUM-IRON PROBLEM

An experiment was performed at the Oak Ridge National Laboratory Tower Shielding Facility (TSF) in 1975-76 to investigate neutron transport from the reactor core to the top deck region of the proposed Clinch River Breeder Reactor (CRBR). Many different arrangements of steel and sodium were studied and extensive analyses of the configurations were performed using both 1-D and 2-D methods. The largest configuration from this experiment was adopted for use in this study and was analyzed using the ANISN[2] 1-D discrete ordinates computer code with several variations in the cross section input. Specifically, numerous trial energy group structures and energy weighting functions were tried, and other cross-section-related parameters such as self-shielding and angular expansion were studied.

Several existing computer programs were utilized for the analyses of the sodium-iron problem and for the generation of the multigroup cross-section libraries. Features of these codes relevant to the present purpose are summarized in the first subsection that follows.

II.1 Computational Procedures

Before the final decisions on the library specifications were made, preliminary multigroup cross-section sets had to be produced for use in the respective analyses. After selecting the final specifications and generating the libraries, testing of the libraries were made on the same sodium-iron problem. Therefore, the analyses of the sodium-iron problem and the generation of the libraries are interwoven, as shown in the flow diagram of the computer runs in Fig. 1. Except for the programs ANISN, AXMIX,[3] and ASPECT,[4] all other codes summarized below are independent modules of the AMPX code system.[5]

The following descriptions of the programs shown in Fig. 1 highlight only features of the codes pertaining to the purpose of the present work:

- AJAX picks a desired set of cross sections from one or more libraries in the AMPX master format and sorts the output cross sections as prescribed.

ORNL-DWG 86-16990

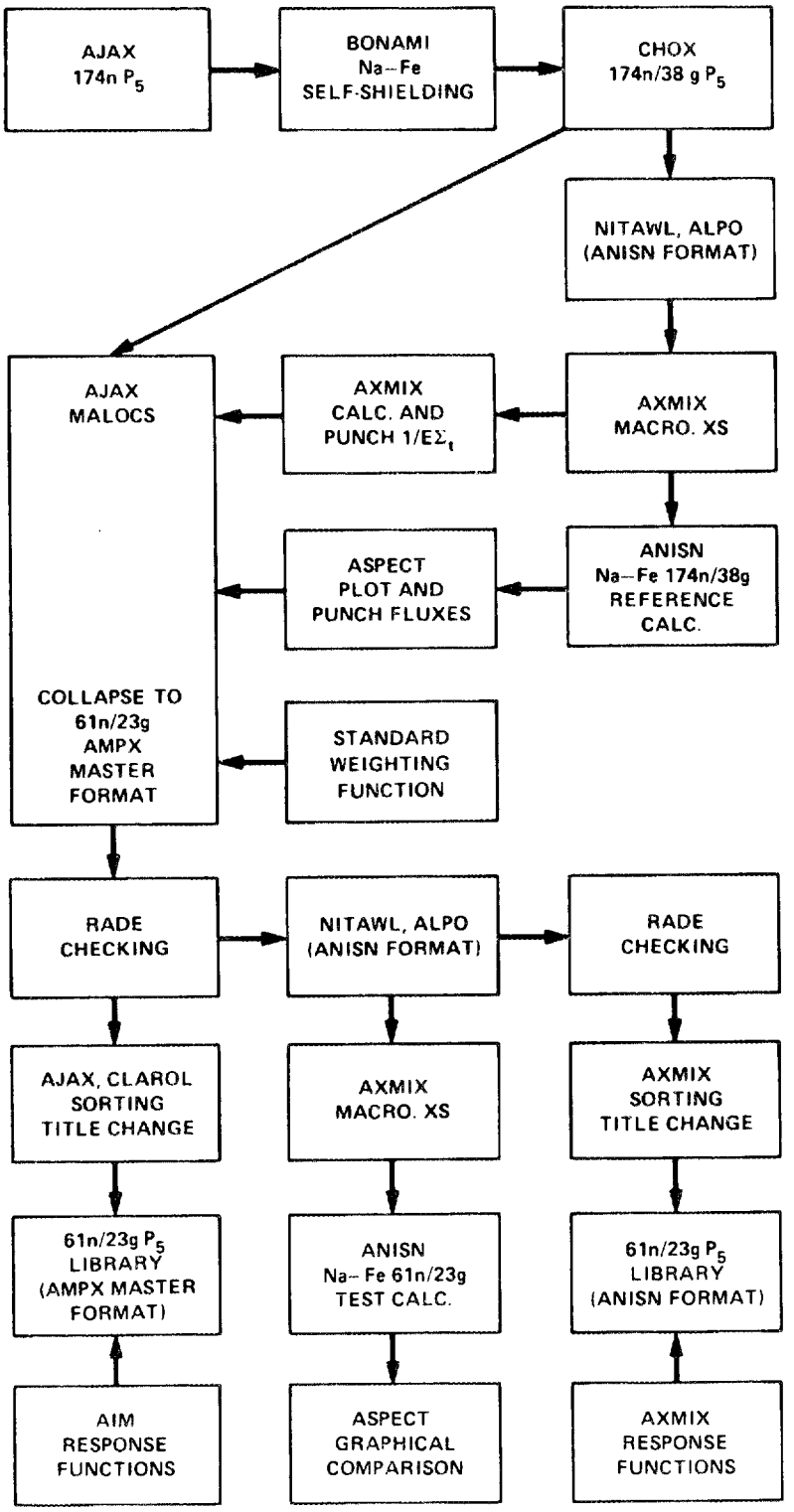

Fig. 1. Computational procedures in selecting the group structures and weighting functions as well as in producing and testing the broad-group cross-section libraries.

- BONAMI performs Bondarenko resonance self-shielding calculations.
- CHOX combines neutron cross sections, gamma-ray production cross sections, and gamma-ray interaction cross sections into coupled sets.
- NITAWL converts cross-section libraries in AMPX master format into AMPX working formats.
- ALPO transforms working libraries generated by NITAWL into the ANISN format.
- AXMIX picks a desired set of cross sections from one or more libraries in the ANISN format and generates macroscopic cross sections. The code was also used to calculate and punch the $1/E\Sigma_t$ weighting functions, to sort and change titles of cross-section sets in the ANISN format, or to convert response functions prepared in BCD format into ANISN binary format.
- ANISN performs 1-D discrete-ordinates coupled neutron-photon transport calculations. The code is capable of collapsing the fine-group macroscopic cross sections into broad groups using zone fluxes, generated internally by ANISN, as the weighting functions. This feature of the code was used in the present work to study the effects of the positions, widths, and numbers of zones for collapsing the fine groups on the calculated results of the sodium-iron problem.
- ASPECT plots and punches neutron and gamma-ray fluxes at any position of the sodium-iron geometry calculated by ANISN. The code was used to generate all the graphical comparisons of various calculated results shown in this report.
- MALOCS collapses fine-group microscopic cross sections in the AMPX master format into specified broad groups using input weighting functions.
- RADE checks the multigroup cross sections processed by various AMPX modules for consistencies among the partial cross sections.
- CLAROL changes titles of cross-section sets in the AMPX master format. For materials having multiple entries in the new libraries, the titles were changed from the original Vitamin-E

titles to identify the differences in weighting functions and compositions. For example, the material iron in the new libraries may have several sets of cross sections - a set generated from the standard weighting, another set generated as a component of stainless steel in $1/E\Sigma_t$ weighting, a third set generated as a component of carbon steel in the self-shielding calculation, etc.

- AIM was used to translate response functions prepared in card image into the AMPX master format and vice versa.

Although Fig. 1 is shown explicitly for the 61n/23γ library, the generation and testing of the 22n/10γ library follow the same computational procedures.

II.2 The Reference 174n/38γ Calculation

The geometry and composition of the sodium-iron problem as well as the results of the ANISN calculation using the Vitamin-E library are described in this section. These results provide a basis for subsequent comparisons of the fine-group data with the various broad group calculations.

The neutron source, representing a typical fast-reactor blanket spectrum, was incident on 31 cm of stainless steel (SS), followed by a small air gap, 4.6 m of sodium housed in 4 aluminum tanks, 1 m of carbon steel, another small air gap, and a LiH reflector region. This geometry is shown in Fig. 2, and also at the bottom of many figures that compare various calculated results as a function of depth into the configuration. The compositions of SS-304, commercial grades of sodium and aluminum, carbon steel, and lithium hydride are listed in Table 1. The Bondarenko factors at 300°K in the Vitamin-E library were used for the self-shielding calculations. The reference ANISN calculation is $S_{16}P_5$. Comparisons of this calculation with a P_3 calculation and a 900°K self-shielding calculation are discussed later in this section. The neutron fluxes per unit lethargy at a number of positions are shown in Figs. 3-5. The corresponding gamma-ray fluxes appear in Figs. 6-8.

ORNL-DWG 86-16989

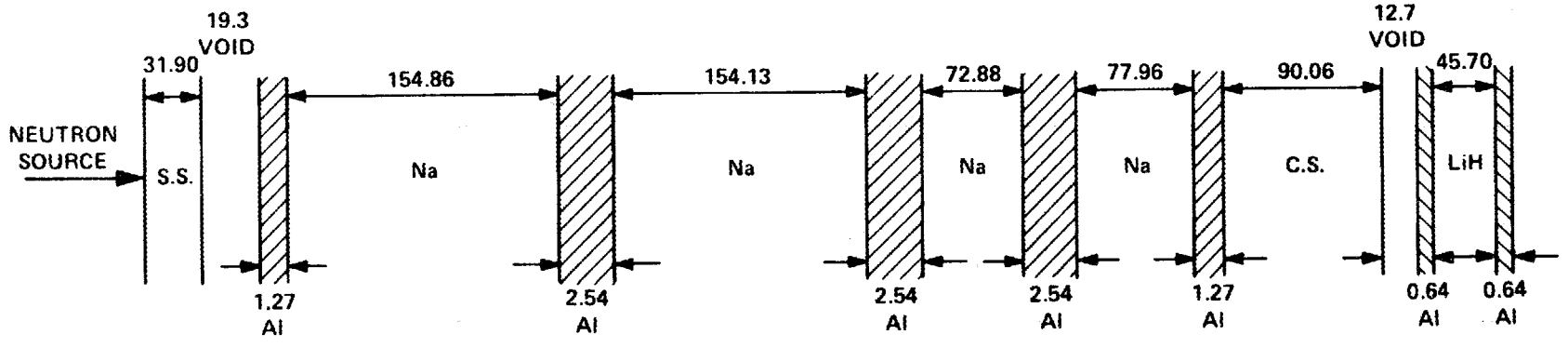

NOTE: ALL DIMENSIONS IN CENTIMETERS. NOT TO SCALE.

Fig. 2. Geometry of the sodium-iron problem.

Table 1. Nuclear Densities of the Materials (in Atoms/Barn-cm)

Elements	Stainless Steel-304	Aluminum	Sodium	Carbon Steel	Lithium Hydride
Fe	5.94(-2)[a]	6.0(-4)	-	8.37(-2)	
Cr	1.69(-2)	-	-	-	-
Ni	7.9(-3)	-	-	-	-
Mn	1.2(-3)	-	-	5.15(-4)	-
C	-	-	-	9.82(-4)	-
H	-	-	2.54(-5)[b]	-	5.61(-2)
O	-	-	3.6(-6)	-	-
Al	-	6.05(-2)	-	-	-
Na	-	-	2.476(-2)	-	-
Ca	-	-	5.7(-6)	-	-
K	-	-	2.2(-6)	-	-
Li[c]	-	-	-	-	5.61(-2)

[a]Read as 5.94×10^{-2}.

[b]Taken to be 75% of the upper limit of 60 ppm for commercial grade sodium.

[c]Natural lithium. For Li^6, multiply by 0.0756; for Li^7, multiply by 0.9244.

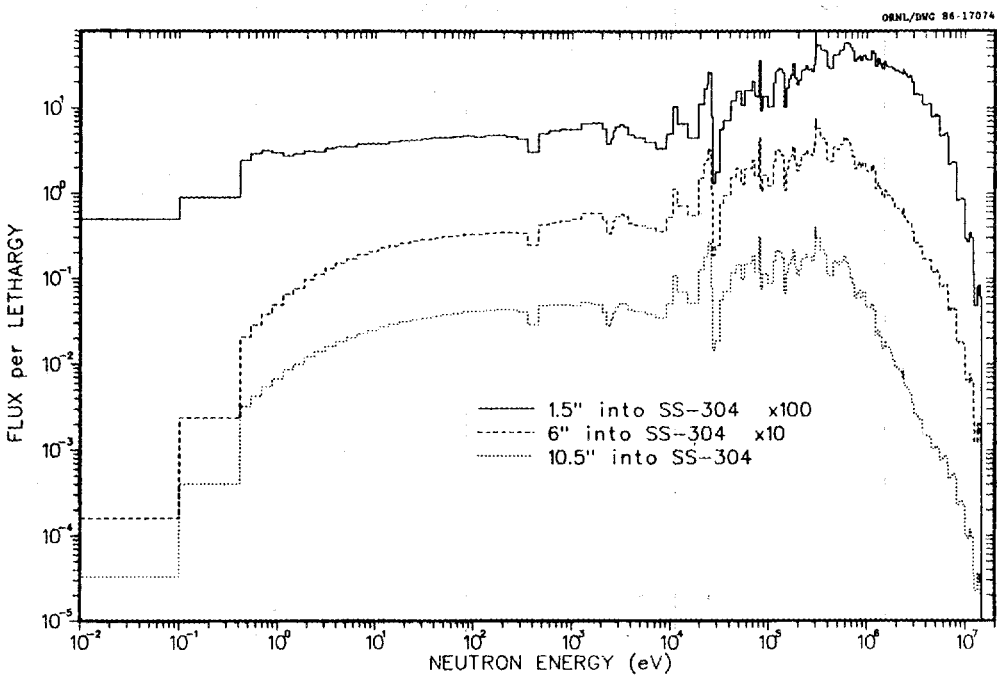

Fig. 3. Changes in the fine-group energy dependence of neutron fluxes through the sodium-iron geometry (stainless steel region).

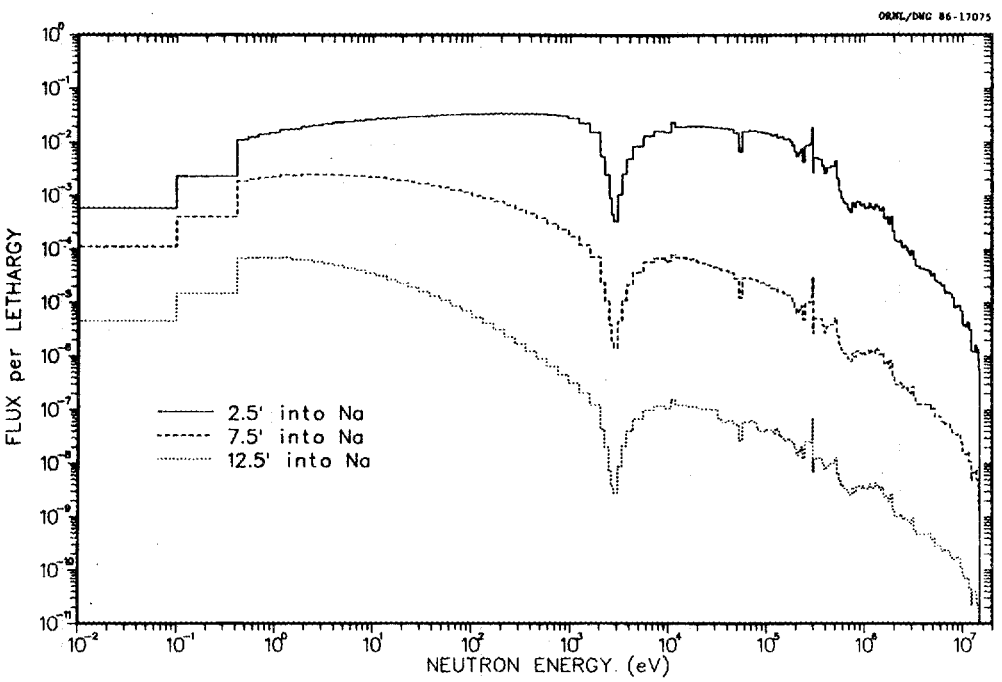

Fig. 4. Changes in the fine-group energy dependence of neutron fluxes through the sodium-iron geometry (sodium region).

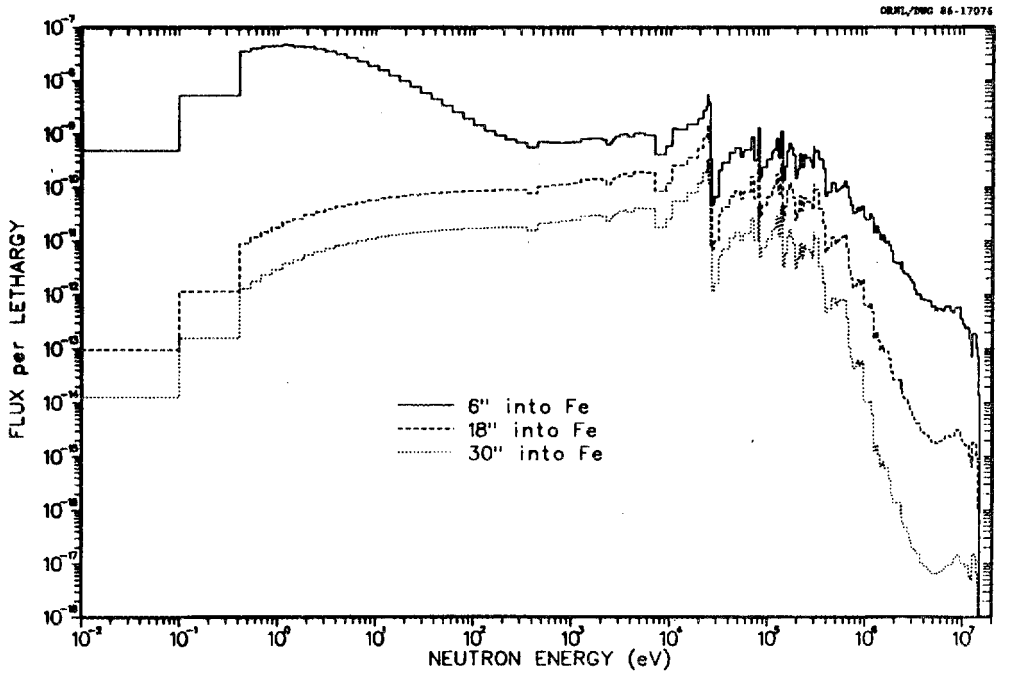

Fig. 5. Changes in the fine-group energy dependence of neutron fluxes through the sodium-iron geometry (carbon steel region).

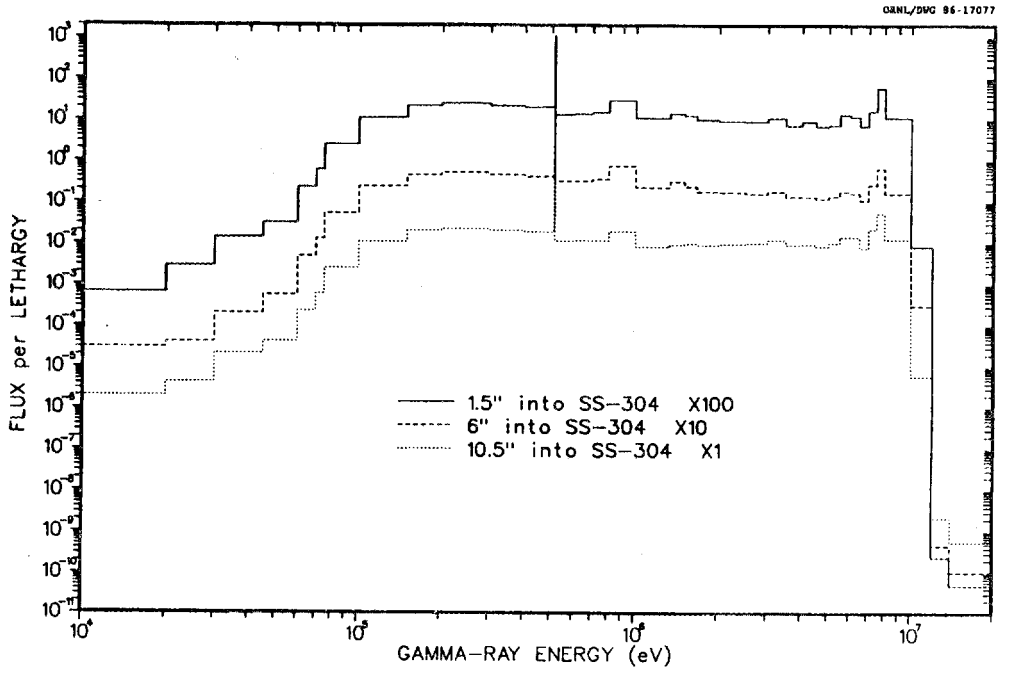

Fig. 6. Changes in the fine-group energy dependence of gamma-ray fluxes through the sodium-iron geometry (stainless steel region).

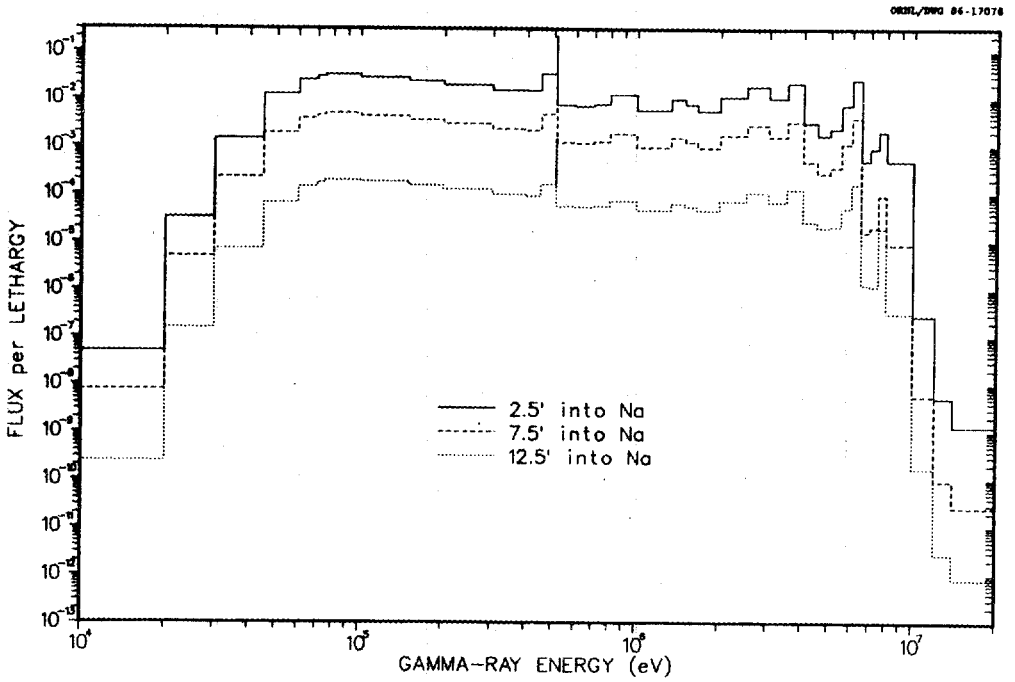

Fig. 7. Changes in the fine-group energy dependence of gamma-ray fluxes through the sodium-iron geometry (sodium region).

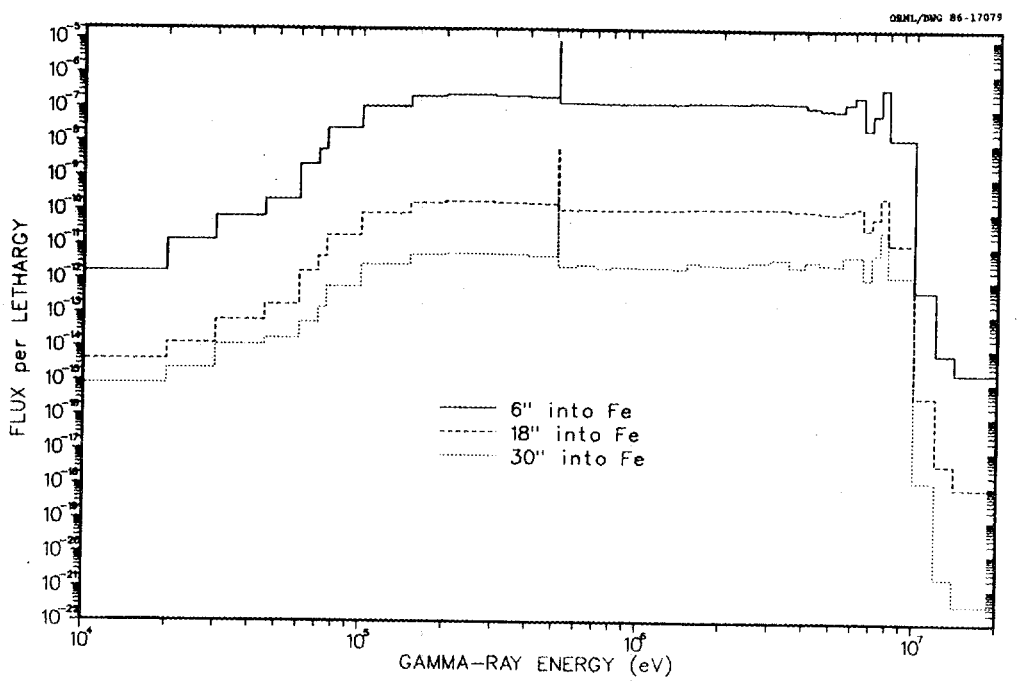

Fig. 8. Changes in the fine-group energy dependence of gamma-ray fluxes through the sodium-iron geometry (carbon steel region).

Examination of the neutron and gamma-ray fluxes shown in Figs. 3-8 reveals several interesting characteristics of neutron penetration through thick sodium-iron shields. First, the energy dependent shapes of the neutron fluxes change significantly as a function of distance into the shield. Looking at the peaks of the neutron spectra, for example, we see that the peak started out near 2 MeV in SS-304, shifted downward in energy by a factor of 10^6 in sodium, then moved back a factor of 10^4 higher in carbon steel. These large changes in the neutron flux shapes imply that a single weighting function for collapsing the fine groups into broad groups cannot be expected to work accurately at all distances into the shield. Secondly, the energy variation in the neutron spectra is the largest just across the boundary of any two media. It can be seen in Fig. 4 that the neutron fluxes in sodium change their shapes more drastically in the initial few feet of sodium than in the remaining several feet. An even larger variation is apparent in Fig. 5 for the fluxes in the front part of the carbon steel. This observation provides some hints as to which and how many spectra should be used to generate position-dependent cross-section sets in the new libraries. Finally, the gamma-ray fluxes shown in Figs. 6-8 exhibit much less variation with energy, position, and medium than the corresponding neutron fluxes. This suggests the probable adequacy in using a single weighting function that is constant in energy for collapsing the fine-group photon cross sections.

Most of the comparisons of different group structures and weighting functions (described in the following sections) were based on integral flux results. This was done by folding the energy-dependent neutron flux with the response of a 4-inch-diameter Bonner ball detector at each mesh point in the calculation and computing the percent difference of the broad-group result relative to the fine-group result. As shown in Fig. 9, the response of the 4-in. ball[6] is representative of total flux (excluding thermal neutrons). Additionally, the neutron flux was integrated over selective energy ranges rather than for the full Bonner ball response. Comparisons of gamma-ray results were based on total flux only.

ORNL/DWG 86-17071

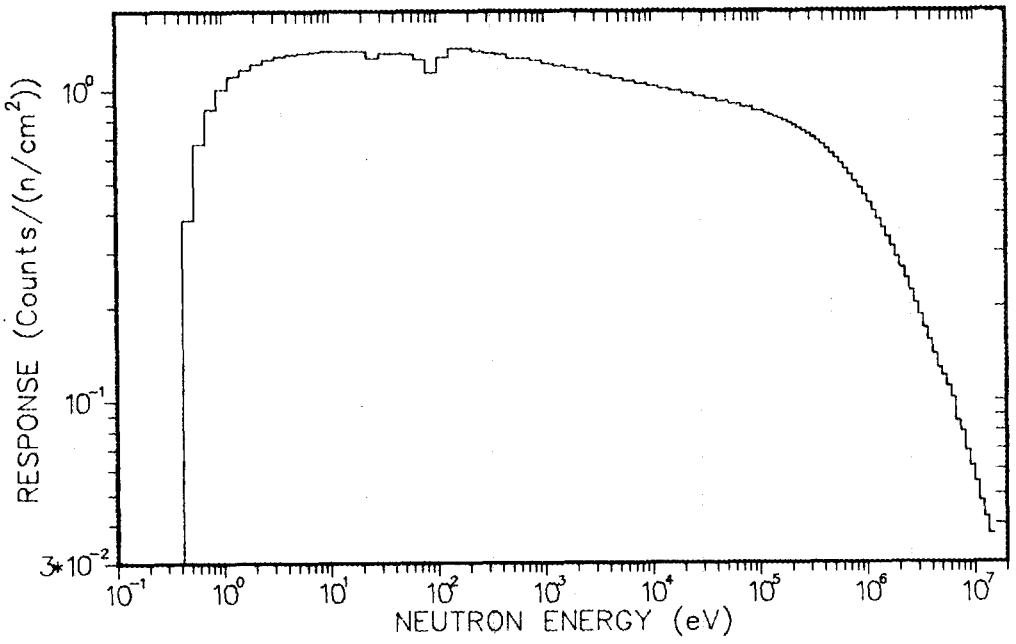

Fig. 9. Response of the 4-inch-diameter Bonner ball detector used as a basis for comparing the different neutron group structures and weighting functions.

II.3 Group Structures

It was recognized at the outset of this study that there was a clear relationship between energy group structures and energy weighting functions. Stated simply: as the number of energy groups increases, the importance of the weighting function decreases. This relationship is particularly important when the transmitted particle flux is changing rapidly with energy such as near cross section windows and resonances. Hence, for a class of problems dominated by only a few materials, it is efficient to use relatively narrow energy groups only in the region of these pronounced structures in the cross sections. It is for this reason that many different broad-group energy group structures have evolved for specific applications.

The present study was started by collapsing the Vitamin-E 174-group neutron cross sections to several different existing broad-group structures. The specific group structures included: (a) the standard 51-group structure used for the last several years at ORNL to analyze LMFBR shielding problems, (b) the 47-group structure used in the BUGLE-80

library[7] for light water reactor shielding problems, and (c) the 45-group PROPANE structure[8] used in France for LMFBR shielding problems. The SS-Na-Fe experiment described in the previous section was analyzed using each of these group structures, and the results were compared with the reference 174-group calculation. These comparisons are shown in Fig. 10 for the 4-in. Bonner ball response.

After comparing the relative performance of the different existing broad-group structures, several new trial group structures were studied.[9] For all of the group structure comparisons, the same flux weighting was used for collapsing to the broad groups. The weighting functions were taken to be the zone-averaged fine-group fluxes in the stainless steel and iron regions and in each of the four sodium tanks.

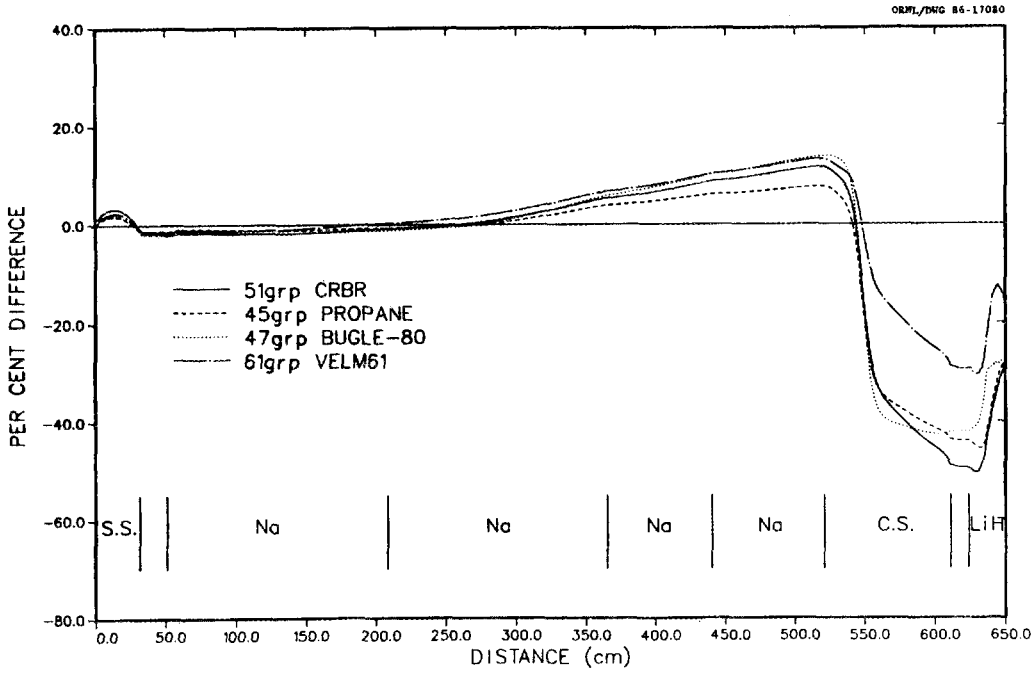

Fig. 10. Comparison of 4-in. Bonner ball responses calculated using fine-group cross sections and various broad-group cross sections collapsed using the same flux weighting.

The study concluded that a group structure containing 61 neutron groups and 23 gamma-ray groups provided acceptable pointwise comparisons with the fine group results as shown in Fig. 10. The energy group boundaries are listed in Tables 2 and 3 compared to the Vitamin-E boundaries, and are shown pictorially in Figs. 11 and 12. It was also decided to construct a few-group library to be used for scoping analyses and higher-dimensional analyses where even 61/23 groups might be impractical. Following a procedure similar to that discussed above, a 22-neutron-group, 10-gamma-ray-group set was selected. The energy boundaries for these structures are also given in Tables 2 and 3 and Figs. 11 and 12. The accuracy of the results computed using these group structures depends heavily on the particular weighting functions used, which are described in the following section.

II.4 Weighting Functions

The energy weighting functions considered for generating the broad-group libraries include: a standard weighting function described below, the $1/E\Sigma_t$ (SS-304) and $1/E\Sigma_t$ (carbon steel) weighting functions, and the neutron fluxes at several positions in the sodium-iron geometry. Effects of these weighting functions on the calculated results as a function of distance into the shield are studied in this subsection. Decisions needed to be made not only on the type of weighting functions, but also on which and how many spectra should be used to generate position-dependent cross-section sets in the new libraries.

Effects of neutron fluxes as weighting functions on the accuracy of the broad-group cross sections can be studied by one of two methods. One method is to use ANISN, which collapses fine-group macroscopic cross sections into broad groups using zone fluxes generated internally as the weighting functions. The resulting broad-group cross-sections sets, one for each zone, are then used in a second ANISN run. The other method is to use some of the neutron fluxes such as shown in Figs. 3-5 as weighting functions in MALOCS to collapse the microscopic cross sections. The former is the preferred method for understanding the problems of weighting functions because the cross sections generated are in macroscopic form and therefore require smaller computer storage. The latter method

Table 2. Broad and Few Group Neutron Structures

Vitamin-E Group	Upper Energy (eV)	61 Group	22 Group	Vitamin-E Group	Upper Energy (eV)	61 Group	22 Group
1	1.9640E 07			46	2.3069E 06		
2	1.7332E 07			47	2.2313E 06	12	
3	1.6905E 07			48	2.1225E 06		
4	1.6487E 07			49	2.0190E 06	13	
5	1.5683E 07			50	1.9205E 06		
6	1.4918E 07	1	1	51	1.8268E 06		
7	1.4550E 07			52	1.7377E 06		
8	1.4191E 07			53	1.6530E 06	14	4
9	1.3840E 07			54	1.5724E 06		
10	1.3499E 07			55	1.4957E 06		
11	1.2523E 07			56	1.4227E 06		
12	1.2214E 07	2		57	1.3534E 06	15	
13	1.1618E 07			58	1.2874E 06		
14	1.1052E 07			59	1.2246E 06		
15	1.0513E 07			60	1.1648E 06		
16	1.0000E 07	3		61	1.1080E 06	16	5
17	9.5123E 06			62	1.0026E 06		
18	9.0484E 06			63	9.6164E 05		
19	8.6071E 06			64	9.0718E 05	17	
20	8.1873E 06	4		65	8.6294E 05		
21	7.7880E 06			66	8.2085E 05		
22	7.4082E 06			67	7.8082E 05		
23	7.0469E 06			68	7.4274E 05	18	6
24	6.7032E 06	5		69	7.0651E 05		
25	6.5924E 06			70	6.7206E 05		
26	6.3763E 06			71	6.3928E 05		
27	6.0653E 06			72	6.0810E 05	19	
28	5.7695E 06			73	5.7844E 05		
29	5.4881E 06	6	2	74	5.5023E 05		
30	5.2205E 06			75	5.2340E 05	20	7
31	4.9659E 06			76	4.9787E 05	21	
32	4.7237E 06			77	4.5049E 05		
33	4.4933E 06	7		78	4.0762E 05		
34	4.0657E 06			79	3.8774E 05	22	8
35	3.6788E 06	8		80	3.6883E 05		
36	3.3287E 06			81	3.3373E 05		
37	3.1664E 06			82	3.0197E 05	23	
38	3.0119E 06	9		83	2.9849E 05	24	9
39	2.8650E 06			84	2.9721E 05	25	
40	2.7253E 06			85	2.9452E 05	26	
41	2.5924E 06			86	2.8725E 05		
42	2.4660E 06	10	3	87	2.7324E 05	27	10
43	2.3852E 06			88	2.4724E 05		
44	2.3653E 06			89	2.3518E 05		
45	2.3457E 06	11		90	2.2371E 05	28	

Table 2. Continued

Vitamin-E Group	Upper Energy (eV)	61 Group	22 Group	Vitamin-E Group	Upper Energy (eV)	61 Group	22 Group
91	2.1280E 05			133	3.3546E 03		
92	2.0242E 05			134	3.0354E 03	45	17
93	1.9255E 05			135	2.7465E 03		
94	1.8316E 05	29		136	2.6126E 03	46	
95	1.7422E 05			137	2.4852E 03		
96	1.6573E 05			138	2.2487E 03	47	
97	1.5764E 05			139	2.0347E 03	48	
98	1.4996E 05	30	11	140	1.5846E 03		
99	1.4264E 05			141	1.2341E 03	49	18
100	1.3569E 05			142	9.6112E 02		
101	1.2907E 05			143	7.4852E 02	50	
102	1.2277E 05	31		144	5.8295E 02		
103	1.1679E 05			145	4.5400E 02	51	
104	1.1109E 05			146	3.5357E 02		
105	9.8037E 04			147	2.7536E 02	52	19
106	8.6517E 04	32	12	148	2.1445E 02		
107	8.2503E 04			149	1.6702E 02	53	
108	7.9499E 04			150	1.3007E 02		
109	7.1998E 04			151	1.0130E 02	54	
110	6.7379E 04			152	7.8893E 01		
111	5.6562E 04	33	13	153	6.1442E 01		
112	5.2475E 04	34		154	4.7851E 01	55	20
113	4.6309E 04			155	3.7267E 01		
114	4.0868E 04			156	2.9023E 01		
115	3.4307E 04	35	14	157	2.2603E 01	56	
116	3.1828E 04			158	1.7603E 01		
117	2.8501E 04	36		159	1.3710E 01		
118	2.7000E 04	37		160	1.0677E 01	57	21
119	2.6058E 04	38	15	161	8.3153E 00		
120	2.4788E 04	39		162	6.4759E 00		
121	2.4176E 04			163	5.0435E 00	58	
122	2.3579E 04	40		164	3.9279E 00		
123	2.1875E 04			165	3.0590E 00		
124	1.9305E 04			166	2.3824E 00	59	
125	1.5034E 04	41		167	1.8554E 00		
126	1.1709E 04			168	1.4450E 00		
127	1.0333E 04			169	1.1253E 00	60	22
128	9.1188E 03	42	16	170	8.7642E-01		
129	7.1017E 03			171	6.8256E-01		
130	5.5308E 03	43		172	5.3158E-01		
131	4.3074E 03			173	4.1399E-01	61	
132	3.7074E 03	44		174	1.0000E-01		
					1.0000E-05		

Table 3. **Broad- and Few-Group Gamma-Ray Structures**

Vitamin-E Group	Upper Energy (eV)	Broad 23 Group	Few 10 Group	Vitamin-E Group	Upper Energy (eV)	Broad 23 Group	Few 10 Group
1	2.0000E 07			21	1.0000E 06	13	6
2	1.4000E 07	1	1	22	8.0000E 05		
3	1.2000E 07			23	7.0000E 05	14	
4	1.0000E 07	2		24	6.0000E 05	15	7
5	8.0000E 06	3	2	25	5.1200E 05		
6	7.5000E 06	4		26	5.1000E 05	16	
7	7.0000E 06	5		27	4.5000E 05		
8	6.5000E 06			28	4.0000E 05	17	
9	6.0000E 06	6	3	29	3.0000E 05	18	8
10	5.5000E 06			30	2.0000E 05		
11	5.0000E 06	7		31	1.5000E 05	19	
12	4.5000E 06			32	1.0000E 05	20	9
13	4.0000E 06	8	4	33	7.5000E 04		
14	3.5000E 06			34	7.0000E 04	21	
15	3.0000E 06	9		35	6.0000E 04		
16	2.5000E 06	10		36	4.5000E 04	22	10
17	2.0000E 06	11	5	37	3.0000E 04		
18	1.6600E 06			38	2.0000E 04	23	
19	1.5000E 06	12			1.0000E 04		
20	1.3300E 06						

ORNL/DWG 86-17072

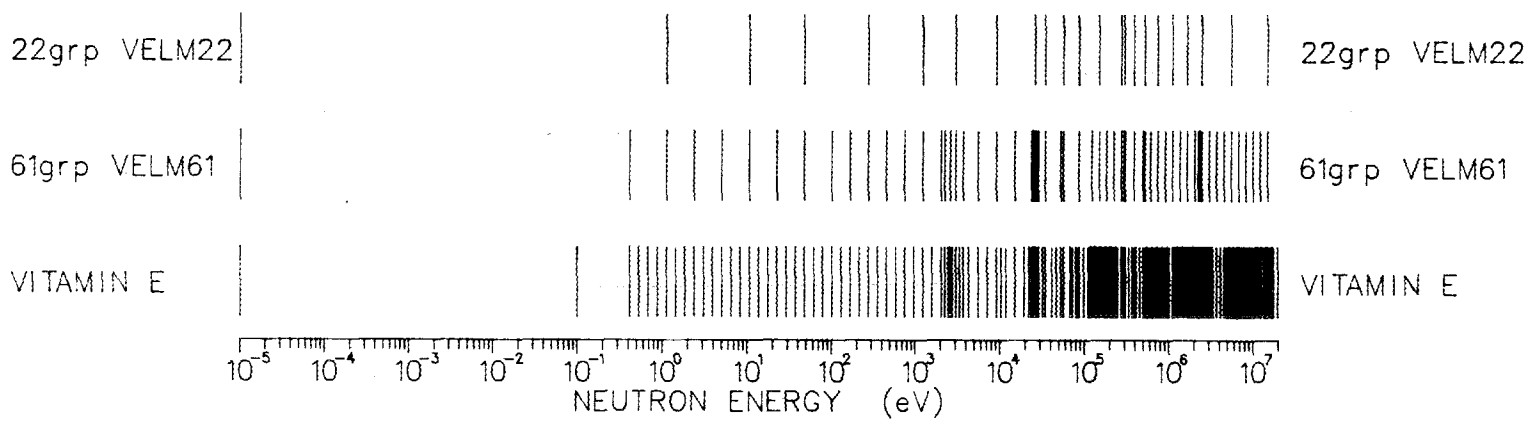

Fig. 11. Comparison of the neutron broad-group boundaries of the VELM61 and VELM22 libraries, listed in Table 2, with the Vitamin-E boundaries.

ORNL/DWG 86-17073

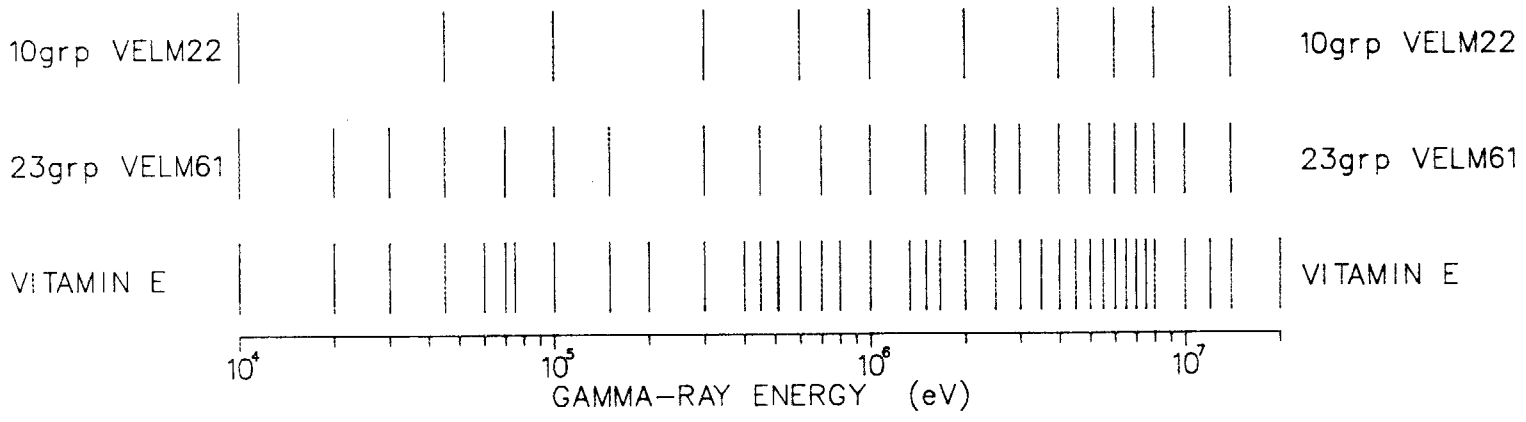

Fig. 12. Comparison of the gamma-ray broad-group boundaries of the VELM61 and VELM22 libraries, listed in Table 3, with the Vitamin-E boundaries.

was used for generating the new libraries for which cross sections in microscopic form are often needed.

In ANISN calculations, a zone is a region of material described by one set of cross sections. The zone flux is the average flux in that zone. The three major components (stainless steel type-304, commercial grade sodium, and carbon steel) in the sodium-iron problem can each be considered as one zone. This definition of zones is referred to in this report as the 1-1-1 zone weighting. Similarly, the sodium in each tank can be treated as one zone, resulting in four sodium zones. This is called the 1-4-1 zone weighting, which was used in II.3 for studying the group structure effects. Calculations using the 61n/23γ cross sections generated in such fashions are compared in Fig. 13 with the reference calculation as percent differences of the 4-in. Bonner ball responses as a function of distance into the shield. It is seen that, in going from

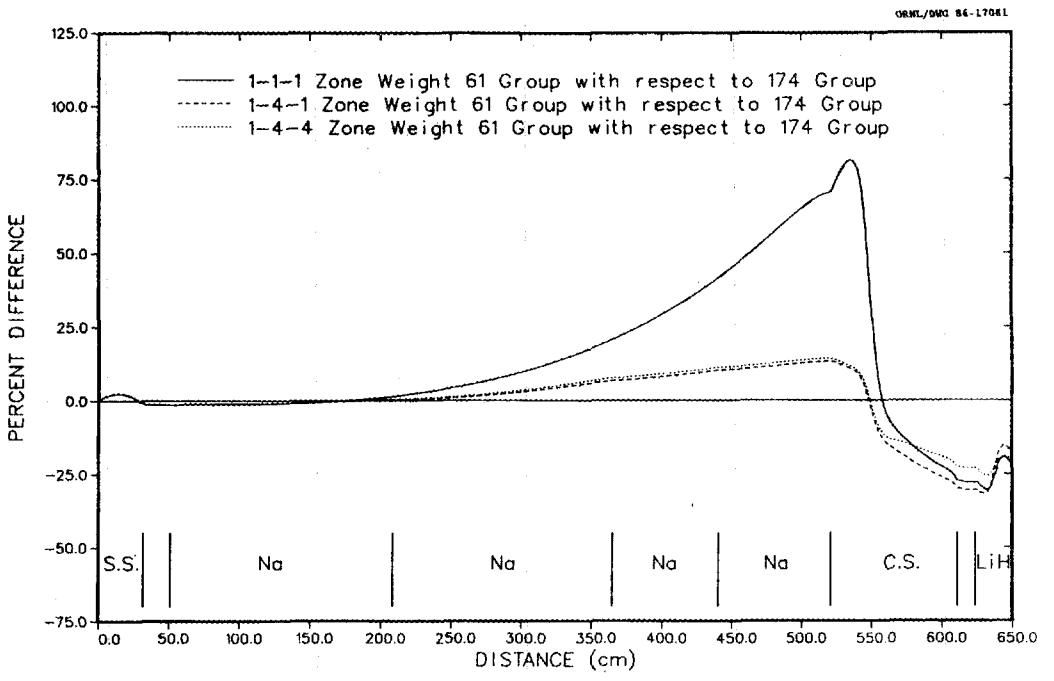

Fig. 13. Comparison of 4-in. Bonner ball responses calculated using fine-group cross sections and 61-group neutron cross sections collapsed using three different zone-averaged weighting functions.

the 1-1-1 weighting to the 1-4-1 weighting, there is substantial improvement in accuracy, particularly at distances deep into sodium. For example, the improvement in accuracy amounts to 70% near the boundary of sodium and carbon steel. The reason for this is a simple one: by treating sodium in all four tanks as one zone, the average flux is dominated by that in the front sodium tank and is thus accurate as a weighting function only for this tank. On the other hand, as can be seen in Fig. 4, the neutron flux in the front sodium tank differs significantly in shape from those in the second, third, and fourth tanks, giving rise to progressively worse results.

We constructed a case designated the 1-4-4 zone weighting by dividing the carbon steel region into four equally spaced zones. Results for this case are also shown in Fig. 13. By increasing the zone number for the carbon steel region from one to four, the improvement in the broad group results is rather small, about 5%. This is puzzling, because the variation in flux shape across carbon steel, shown in Fig. 5, is quite large, suggesting a large improvement in accuracy in the broad group results when four zones are used instead of one. A second inexplicable phenomenon is also seen in Fig. 13. Regardless of agreement or disagreement in the Bonner ball responses near the boundary of sodium and carbon steel, the broad-group results in the three cases always come close at distances between 30 cm and 100 cm into carbon steel.

Dividing the second tank of sodium into two zones and using the broad-group cross sections of the second of these two zones for all four tanks of sodium, we constructed a special case of zone weighting labeled 1-1M-1. This 1-1M-1 zone weighting represents a case for which SS-304 is considered as one zone, sodium in all four tanks as another zone but the neutron flux near the middle of this zone is used as the weighting function, and carbon steel as the third zone. Calculated results for this case are compared in Fig. 14 with the reference calculation in terms of percent differences of the 4-in. Bonner ball responses verses distance. It is seen that the improvement in accuracy in the broad group results of the 1-1M-1 weighting over that of the 1-1-1 weighting is substantial and comparable to that achieved in the case of the 1-4-1 zone weighting shown in Fig. 13. However, an extension of the 1-1M-1 case to 1-1M-1M, by treating carbon steel in a manner similar to that described above for

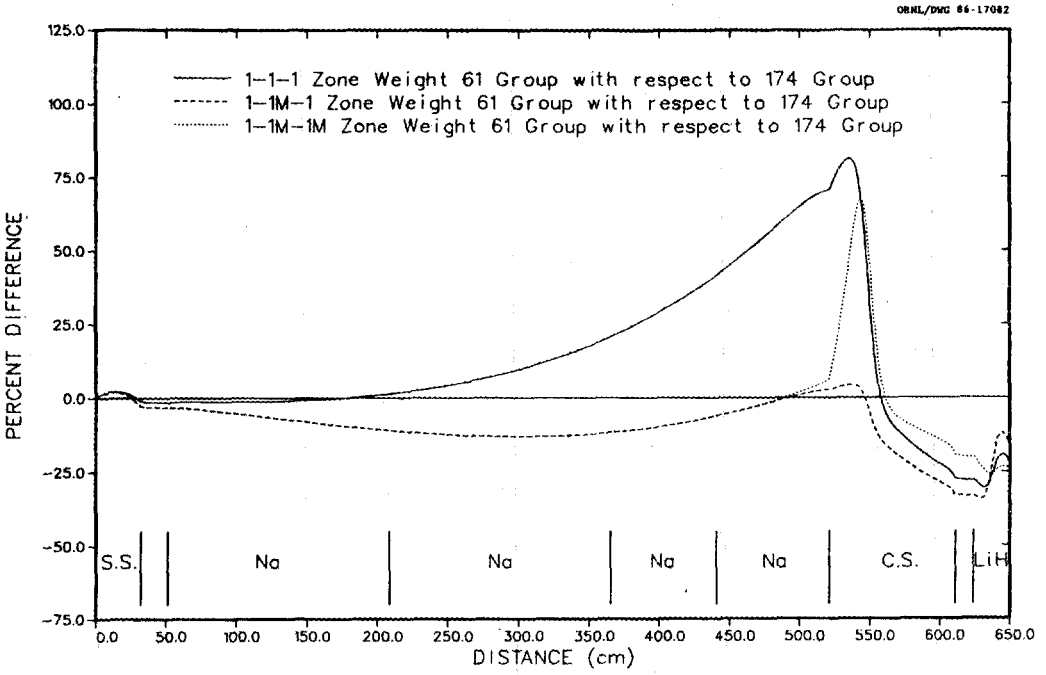

Fig. 14. Comparison of 4-in. Bonner ball responses calculated using fine-group cross sections and 61-group neutron cross sections collapsed using three different modified zone-averaged weighting functions.

sodium, ended up in less favorable comparisons, also shown in Fig. 14. These conflicting results seem to be due to the fact that the flux at the middle of the sodium region represents a good average for the whole sodium region, while the flux at the middle of the carbon steel region does not. As seen in Fig. 5, the shape change in fluxes from the front part of the carbon steel region to the middle part is quite large, with a reverse in energy dependence in a good part of the energy range. This observation suggests that a zone of carbon steel about 30-cm-thick behind sodium should be considered separately.

From the zone weighting studied above, it is apparent that the location from where the flux is taken and used as the weighting function for the whole zone can be important. It is also clear that the widths and numbers of zones for a given material can make significant differences in the broad-group results. Other cases of zone weighting were studied and are summarized below:

1. A broad group calculation with a 1-10-1 weighting yielded 4-in. Bonner ball responses within 3% of the reference calculation in the sodium region.

calculation in the sodium region.

2. A 1-3M-1 case is comparable in accuracy to the 1-10-1 case.
3. The 2-4-1 results agree with 1-4-1 within 1% throughout the sodium-iron geometry.
4. The 1-4-2 results agree with 1-4-4 within 2%.
5. Similar but less extensive studies were made for some 22n/10γ calculations. Problems in the 22n/10γ results are similar to those in the 61n/23γ calculations but are quantitatively magnified by up to five times.
6. Problems in the calculated broad-group total gamma-ray fluxes are similar to the corresponding 4-in. Bonner ball responses but are generally much less severe.

The lessons learned above can now be applied to the generation and the application of the position-dependent broad-group cross-section sets in the new libraries:

1. The steel region near the reactor core can be considered as one zone. The neutron flux a few centimeters from the source can be used as the weighting function.
2. The sodium region should be treated as three zones. The neutron fluxes near the middle of each zone should be used as the weighting functions. For a problem with a less thick sodium region, the cross sections generated for the front one or two zones in the present problem can be used.
3. The carbon steel region can be considered as two zones. The front zone should be about 30-cm-thick regardless of the total thickness of the carbon steel region. The neutron fluxes near the middle of each zone should be used as the weighting functions. If one zone is desired, the cross sections for the front zone in the two-zone approximation can be adequately used.

The above conclusions lead to the 1-3-2 flux weighting referred to in Figs. 15-18 and used for generating part of the broad group libraries. Specifically, the SS-304 zone employed the 3.8-cm flux (1.5-in.) as the

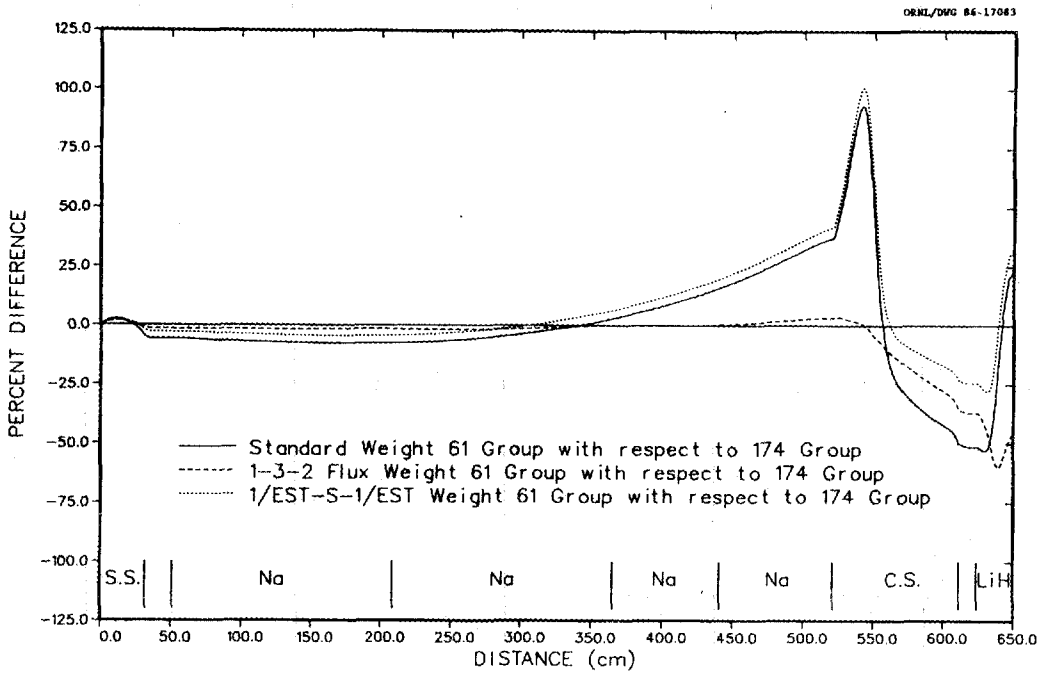

Fig. 15. Comparison of 4-in. Bonner ball responses calculated using fine-group cross sections and 61-group neutron cross sections collapsed using three final weighting functions.

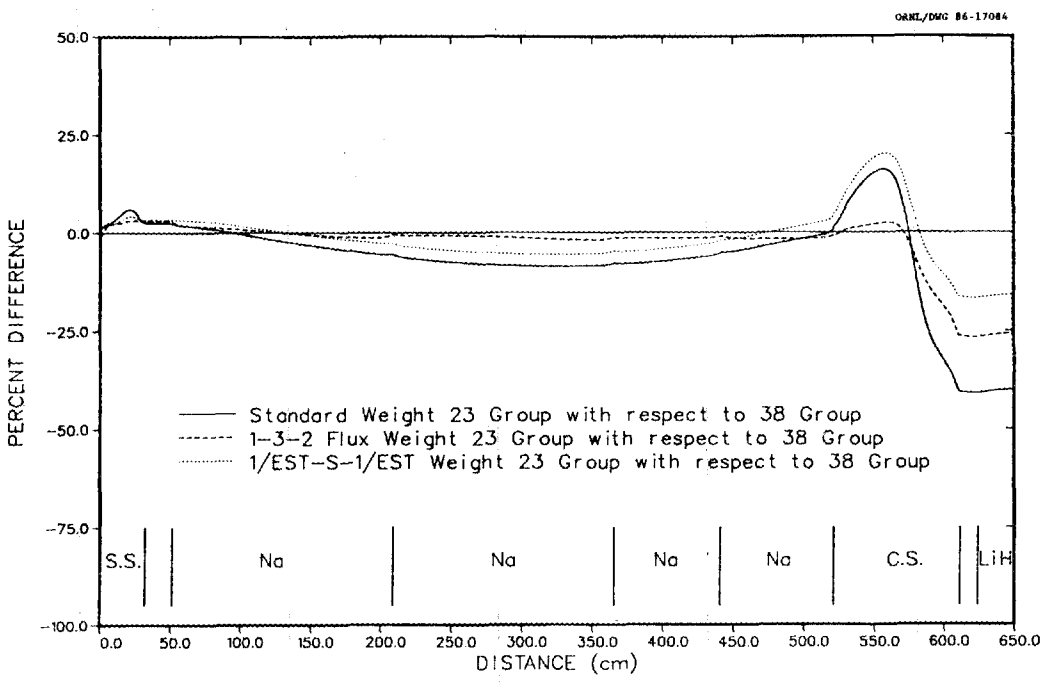

Fig. 16. Comparison of total gamma-ray fluxes calculated using fine-group cross sections and 61-group neutron cross sections collapsed using three final weighting functions. Note: Gamma-ray weighting is flat.

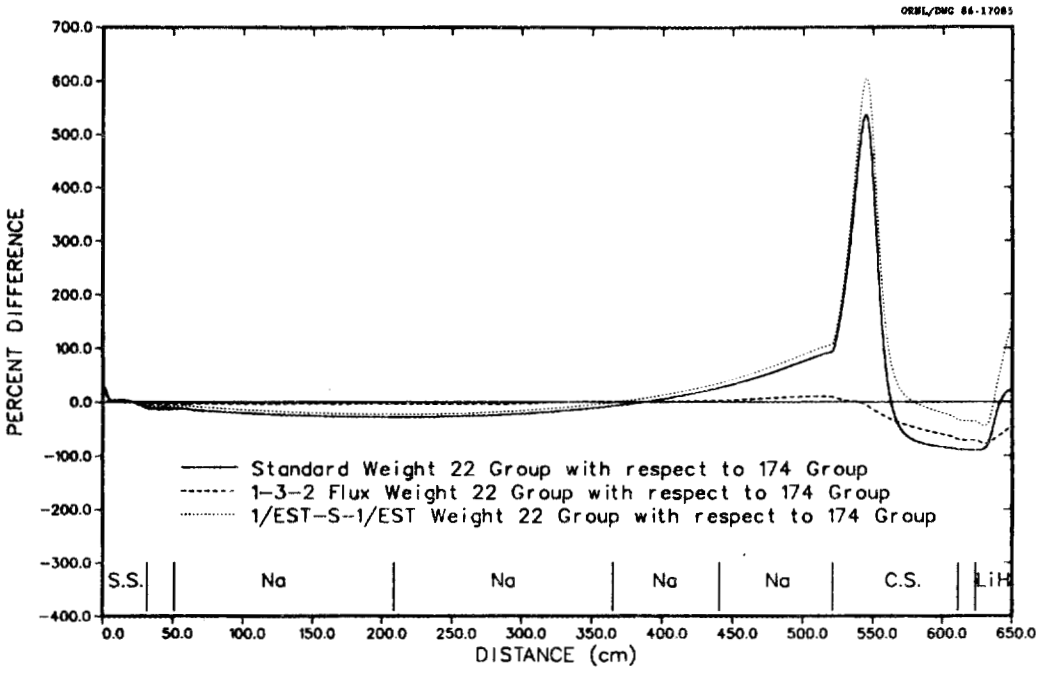

Fig. 17. Comparison of 4-in. Bonner ball responses calculated using fine-group cross sections and 22-group neutron cross sections collapsed using three final weighting functions.

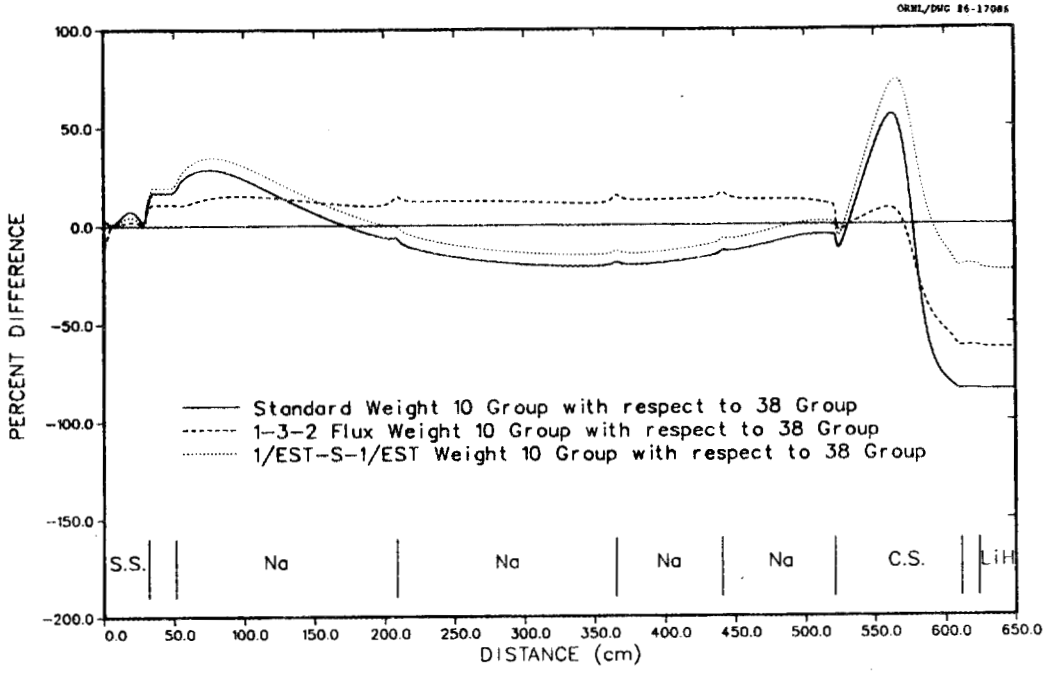

Fig. 18. Comparison of total gamma-ray fluxes calculated using fine-group cross sections and 22-group neutron cross sections collapsed using three final weighting functions. Note: Gamma-ray weighting is flat.

weighting function; the fluxes at the middle of each of three equally spaced zones were used for the sodium region; and the flux at 15 cm (6-in.) in carbon steel was used for the front 30-cm-thick zone and the flux at 45 cm (18-in.) was used for the back zone. All these fluxes appear in Figs. 3-5. The techniques used for generating and testing this part of the libraries are shown in Fig. 1 and discussed in subsection II.1. We now describe the other two types of weighting functions - the standard weighting function and the $1/E\Sigma_t$ weighting function, and compare the differences of the three types of weighting functions via the sodium-iron problem.

The standard weighting function referred to in this report was derived from the Vitamin-E weighting function by removing its fusion peak. The resulting weighting function takes the following form:

1. Maxwellian thermal spectrum 10^{-5} eV to 0.414 eV

$$C_1 E e^{-E/kT}$$

2. 1/E slowing down spectrum 0.414 ev to 2.12 MeV

$$C_2/E$$

3. Fission spectrum 2.12 MeV to 10 MeV

$$C_3 E^{\frac{1}{2}} e^{-E/(1.415\ \mathrm{MeV})}$$

4. 1/E spectrum 10 MeV to 15 MeV

$$C_4/E$$

The $1/E\Sigma_t$ (SS-304) and $1/E\Sigma_t$ (carbon steel) weighting functions are often used for the steel regions in many shielding problems. These weighting functions give a favorable bias to the fine resonance windows apparent in the neutron spectra in stainless steel and carbon steel shown respectively in Figs. 3 and 5. Due to the extra $1/\Sigma_t$ bias, the broad-group cross sections are expected to be smaller than those generated using the standard weighting function, which is essentially 1/E for the sodium-iron problem.

Results of the 61n/23γ calculations for the sodium-iron problem using the three types of weighting functions are compared in Fig. 15 with the 174n/38γ calculation as percent differences of the 4-in. Bonner ball responses verses distance. The corresponding results for the total gamma-ray fluxes are shown in Fig. 16. Figures 17 and 18 are similar comparisons for the 22n/10γ calculations. The label 1/EST-S-1/EST in these four figures stands for $1/E\Sigma_t$ (SS-304)-Standard-$1/E\Sigma_t$ (carbon steel) for the three major zones. From Figs. 15-18, it is seen that the results for the standard weighting and the $1/E\Sigma_t$ weighting are similar in characteristics but the latter is larger, reflecting the $1/E\Sigma_t$ bias that increases neutron penetration through the shield. Both types of weighting yielded rather poor results at a distance 18 cm into carbon steel while the 1-3-2 flux weighting gave much improved results, particularly for the 22n/10γ calculations.

II.5 Additional Library Specifications

Decisions regarding resonance self-shielding, temperature, and order of Legendre expansion for the new libraries were made based on considerations described below.

II.5.a Resonance Self-Shielding

A calculation similar to the reference 174n/38γ calculation was run using cross sections that were not self-shielded. This calculation is compared in Fig. 19 with the reference calculation as percent differences of the 4-in. Bonner ball responses verses distance. When self-shielding is ignored, resonance absorption increases and the total neutron fluxes decrease throughout the shield, particularly in the carbon steel. For example, the 4-in. Bonner ball responses calculated for a position immediately behind carbon steel differ by 50%. Therefore, cross-section sets with resonance self-shielding for the constituents of SS-304, commercial grades of sodium and aluminum, carbon steel, and lithium hydride are also included in the broad group libraries. The cross sections of the constituents of the self-shielded SS-304 can be used for SS-316 also

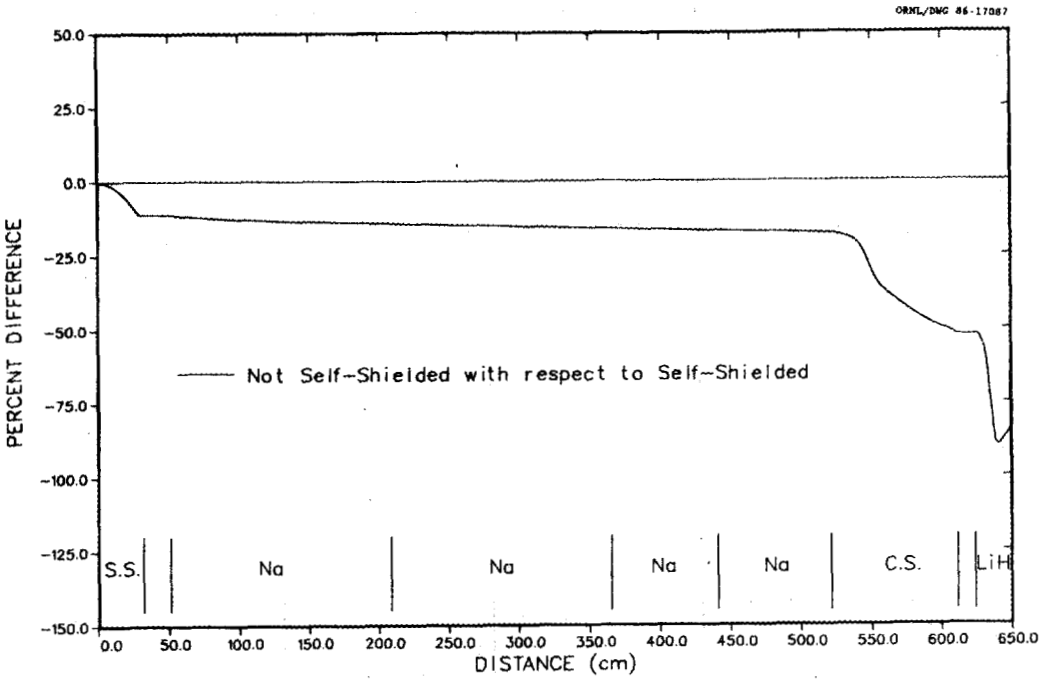

Fig. 19. Comparison of 4-in. Bonner ball responses calculated using fine-group cross sections with and without resonance self-shielding.

because the differences in composition between SS-304 and SS-316 are not large. This last point is discussed further in Section III regarding the inclusion of molybdenum, a constituent of SS-316, in the new libraries. For a similar reason, the cross sections of iron as a component of self-shielded carbon steel are good approximations for self-shielded iron. Since cross sections without self-shielding are also given in the new libraries, the user may opt to omit self-shielding in some of the materials such as the commercial grade sodium, for which self-shielding has a rather small effect.

II.5.b Temperature

Another calculation similar to the reference 174n/38γ calculation employed the Bondarenko factors at 900°K, instead of 300°K, for the self-shielding calculation. This calculation is compared in Fig. 20 with the reference calculation as percent differences of the 4-in. Bonner ball

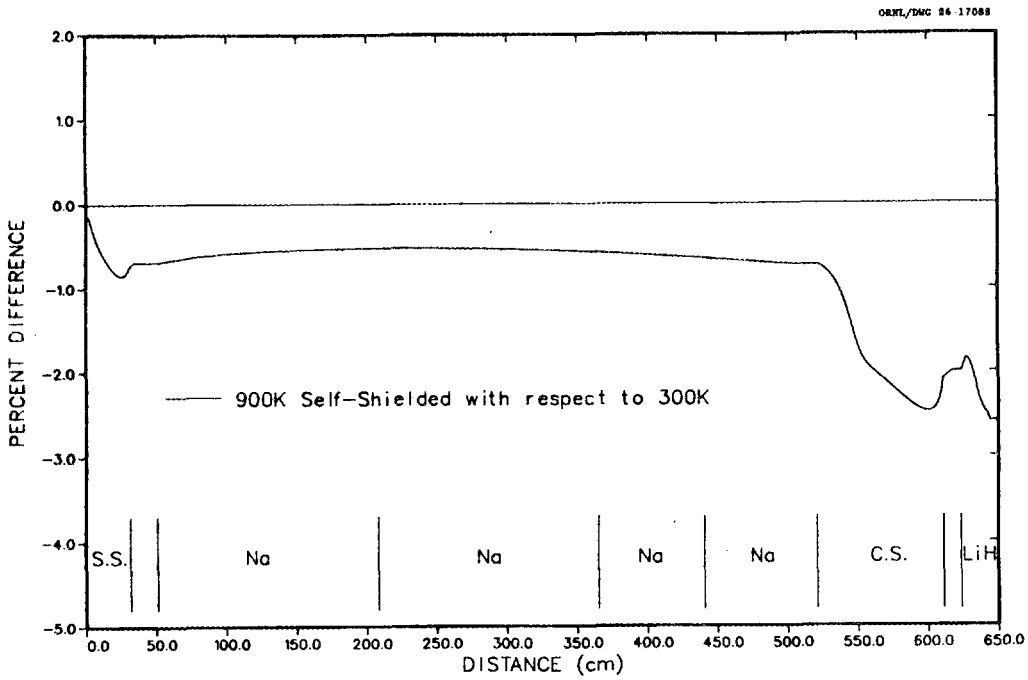

Fig. 20. Comparison of 4-in. Bonner ball responses calculated using fine-group cross sections self-shielded at 900°K and 300°K.

responses verses distance. The differences are quite small (less than 3%) compared with the other effects shown in this section. Therefore, the new libraries only contain cross sections self-shielded at 300°K.

II.5.c Legendre Order

A third calculation similar to the 174n/38γ reference had cross sections expanded in P_3, instead of P_5. The differences between this calculation and the reference calculation are shown in Fig. 21 as before. The differences are not large (about 5%) compared with the other effects already discussed. However, because P_5 expansion is generally known to be necessary for gamma-ray interactions, we generated the new libraries in P_5 expansion. In case a user prefers to use P_3, it is a simple matter to read only the P_3 parts of the libraries.

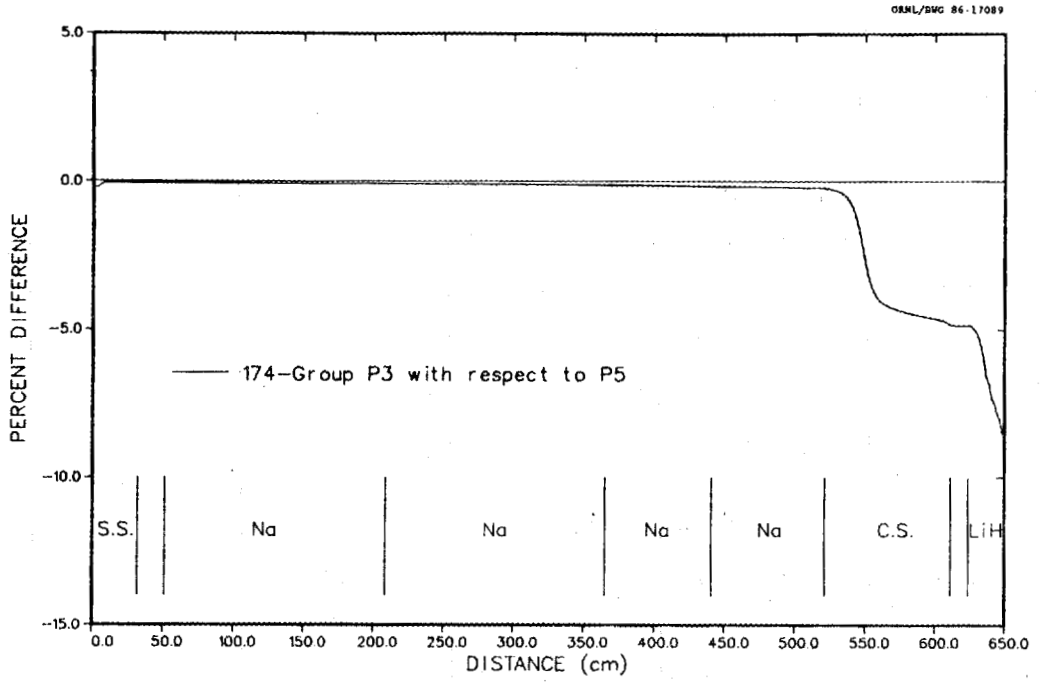

Fig. 21. Comparison of 4-in. Bonner ball responses calculated using fine-group cross sections with P3 angular expansion and P5 expansion.

III. CONTENTS OF THE LIBRARIES

The contents of the VELM61 and VELM22 libraries, the identifications of the materials, and other clarifications are presented in Section III.1. A large variety of response functions presently available in other libraries were converted into the structures of the present libraries, as explained in Section III.2.

III.1 The Cross Section Libraries

All elements and isotopes in the Vitamin-E library available as of August 20, 1985 are included in the first part of the new libraries and were generated using the standard weighting function. This part is listed in Table 4. Some of the redundant entries in the Vitamin-E library are retained in the new libraries for reasons given below. The redundant entries retained are ^{1}H, ^{9}Be, ^{11}B, and Zr. The older entry for ^{1}H, with ID = 9301 in the AMPX master format, is the one used in the analyses of the sodium-iron problem. The newer version of ^{1}H, with ID = 930101, became available after most of the sodium-iron analyses had been completed. This version had a processing philosophy in the thermal region slightly different from that used for the older version. Hence both versions are kept. The extra entry for ^{9}Be, with ID = 104 in the AMPX master format, is retained because this entry is considered a viable alternative to the corresponding ENDF/B-V entry,[10] ID = 130401. The other two redundant materials, from sources other than ENDF/B-V, are retained because the corresponding ENDF/B-V entries do not have gamma-ray production cross sections. Though these extra entries do have gamma-ray production cross sections, it is not certain that their neutron cross sections are better than those in ENDF/B-V. Therefore, both versions are adopted in the new libraries. The redundant materials in the Vitamin-E library excluded from the new libraries are all obsolete Mod-1 versions of ENDF/B-V which include ^{7}Li, ^{40}Ca, ^{55}Mn, Fe, ^{59}Co, Ni, ^{181}Ta, and Pb. The identifications of the cross sections in the AMPX master format listed in Table 4 are identical to those in the Vitamin-E library. The identifications in the ANISN format are ordered according to the atomic mass numbers.

Table 4. Materials in the VELM61 Libraries with Standard Weighting

Material	ID (AMPX)	ID (ANISN)	Material	ID (AMPX)	ID (ANISN)
H-1	9301	1-6	Sn	8850	247-252
H-1	930101	7-12	Cs-137	966901	253-258
H-2	930202	13-18	Ba-138	135301	259-264
H-3	116901	19-24	Gd	8853	265-270
He-4	127000	25-30	Hf-174	137401	271-276
Li-6	130301	31-36	Hf-176	137601	277-282
Li-7	139701	37-42	Hf-177	137701	283-288
Be-9	130401	43-48	Hf-178	137801	289-294
Be-9	104	49-54	Hf-179	138301	295-300
B-10	130501	55-60	Hf-180	138401	301-306
B-11	116000	61-66	Ta-181	128502	307-312
B-11	8811	67-72	W-182	182	313-318
C	130601	73-78	W-183	183	319-324
N-14	127501	79-84	W-184	184	325-330
O-16	127601	85-90	W-186	186	331-336
F-19	130902	91-96	Re-185	108301	337-342
Na-23	131101	97-102	Re-187	108401	343-348
Mg	131201	103-108	Au-197	8861	349-354
Al-27	131301	109-114	Pb	138202	355-360
Si	131401	115-120	Bi-209	137501	361-366
P-31	131501	121-126	Th-232	139001	367-372
S	134701	127-132	Pa-233	139101	373-378
Cl	114901	133-138	U-233	139301	379-384
Ar	8824	139-144	U-234	9394	385-390
K	115001	145-150	U-235	139501	391-396
Ca	132003	151-156	U-236	139601	397-402
Ti	132201	157-162	U-238	139801	403-408
V	132301	163-168	Np-237	133701	409-414
Cr	132401	169-174	Pu-238	133801	415-420
Mn-55	132502	175-180	Pu-239	139901	421-426
Fe	132603	181-186	Pu-240	138001	427-432
Co-59	132703	187-192	Pu-241	138101	433-438
Ni	132802	193-198	Pu-242	134201	439-444
Cu	132901	199-204	Am-241	136101	445-450
Ga	135801	205-210	Am-242	854201	451-456
Y-89	920201	211-216	Am-242M	136901	457-462
Zr	134002	217-222	Am-243	136301	463-468
Zr	8841	223-228	Cm-242	864201	469-474
Nb-93	118901	229-234	Cm-243	134301	475-480
Mo	132101	235-240	Cm-244	134401	481-486
Cd	8847	241-246			

Contents of the second part of the libraries are listed in Table 5. This part of the libraries includes elements and isotopes used in the analyses of the sodium-iron problem, plus molybdenum, a constituent of SS-316. The identifications of all entries in Table 5 are different from those in Table 4 since both tables contain parts of the same libraries. However, the identifications in the VELM61 and VELM22 libraries are identical. More specifically, a user can access four separate libraries:

1. A 61n/23γ library in the AMPX master format containing materials listed in Tables 4 and 5.
2. A 61n/23γ library in the ANISN format containing materials listed in Tables 4 and 5.
3. A 22n/10γ library in the AMPX master format containing materials listed in Tables 4 and 5.
4. A 22n/10γ library in the ANISN format containing materials listed in Tables 4 and 5.

The materials in Table 5 appear in three groups according to the three types of weighting functions used for their creation. The cross sections in the first group were generated using the standard weighting function to collapse self-shielded cross sections, resulting in composition-dependent materials. For example, there are three entries for iron in this group: one as a constituent of SS-304, another as a part of commercial grade aluminum, and the third as a component of carbon steel. The cross sections in the second group in Table 5 were generated using the flux weighting defined in subsection II.4. Among the constituents of commercial grade sodium and carbon steel, only sodium and iron are included in this group. The cross sections of other constituents of commercial grade sodium and carbon steel can be taken from the first group for use in the second group without making any significant differences in the calculated results. This has been confirmed by testing. The cross sections in the third group in Table 5 were generated using the $1/E\Sigma_t$ weighting function. For the $1/E\Sigma_t$ (carbon steel) weighting, only the inclusion of iron was considered necessary.

Table 5. Materials in the VELM61 and VELM22 Libraries used in the Na-Fe Calculations

Material	ID (AMPX)	ID (ANISN)	Description
		(Standard Weighting, Self-Shielded)	
Fe	132611	501-506	
Cr	132411	507-512	Constituents of SS-304
Ni	132811	513-518	
Mn-55	132511	519-524	
Fe	132612	525-530	Constituents of Al
Al-27	131311	531-536	
H-1	9311	537-542	
O-16	127611	543-548	
Na-23	131111	549-554	Constituents of Na
Ca	132011	555-560	
K	115011	561-566	
Fe	132613	567-572	
Mn-55	132512	573-578	Constituents of Carbon Steel
C	130611	579-584	
H-1	9312	585-590	
Li-6	130311	591-596	Constituents of LiH
Li-7	139711	597-602	
		(Na-Fe Interval-Flux Weighting)[a]	
Fe	132621	603-608	
Cr	132421	609-614	Flux 3.8-cm into SS-304
Ni	132821	615-620	
Mn-55	132521	621-626	
Mo	132121	627-632	
Na	131121	633-638	Flux 76.2-cm into Na
Na	131122	639-644	Flux 228.6-cm into Na
Na	131123	645-650	Flux 381.0-cm into Na
Fe	132622	651-656	Flux 15.2-cm into Carbon Steel
Fe	132623	657-662	Flux 45.7-cm into Carbon Steel
		($1/E\Sigma_t$ Weighting)	
Fe	132631	663-668	
Cr	132431	669-674	
Ni	132831	675-680	$1/E\Sigma_t$(SS-304)
Mn-55	132531	681-686	
Mo	132131	687-692	
Fe	132632	693-698	$1/E\Sigma_t$ (Carbon Steel)

[a]Designated as the 1-3-2 flux weighting in Section II.4.

Molybdenum is also included in the last two groups of materials in Table 5. This allows approximate calculations of the macroscopic cross sections of SS-316 under all three types of weighting without generating too many cross-section sets. For example, to calculate the macroscopic cross sections of SS-316 using the flux weighting, one can take the cross sections of Fe, Cr, Ni, Mn, and Mo from the second group of Table 5 and the cross sections of Si and C from those in Table 4. Though a small error will result, this error is not likely to exceed the concentration of Si and C in SS-316 which is 1%.

The weighting function for the gamma-ray interaction cross sections was assumed to be constant in energy.

In the Vitamin E library, cross sections for most of the light elements and the primary constituents of common structural materials are provided with a P_8 Legendre expansion of the scattering cross sections. The primary fissile materials are given with a P_5 expansion, and the remaining lesser important materials are given with only a P_3 expansion. It was decided to generate the VELM libraries with a P_5 Legendre expansion due to the perceived importance of using P_5 for some deep penetration problems and especially for gamma-ray transport problems. This implies that the P_4 and P_5 scattering coefficients are padded with zeros for those few materials which only contained P_3 expansion in Vitamin E.

III.2 The Response Functions

A large variety of response functions presently available in other libraries were converted, by interpolation or collapsing as explained below, into the structures of the present libraries. The availability of these response functions in the same group structures as those of the cross-section libraries should prove to be most convenient to the users of the present libraries. However, it should be pointed out that some of the responses are based on data predating the ENDF/B-V version, such as the heating functions derived from the MACKLIB-IV KERMA factors[11] which may need to be updated.

The response functions in the ANISN format are given as one material (ID=1000) in the form of an "activity table" for VELM61 and two materials (ID=1000 and 2000) for VELM22. For each table position, the number of

entries is always the total number of groups, regardless of whether the response function is for neutron only, for gamma-ray only, or for both. The response functions are listed in Table 6, which also gives their corresponding table positions in the VELM61 activity table (ID = 1000).

For VELM22 in the ANISN format, the first material (ID=1000) contains the first 33 responses listed above, the second material (ID=2000) the last 35. In other words, the first table position in ID = 2000 contains the iron total heating.

For both VELM61 and VELM22 in the AMPX master format, the above response functions are given as a one-dimensional array in material 1000. In this one-dimensional array, each response function is preceded by an identifier, referred to as the MT number, which is 9000 plus the table position listed above. For example, MT = 9014 is the identifier for the 4.03-in. Bonner ball response. Note that in the AMPX master format redundant data, i.e. data which can be derived from other existing data, are not allowed. Therefore, responses which merely combine the individual neutron and gamma-ray responses (responses 7, 20, 34, 37, 40, and 43) are omitted from the AMPX activity material.

The first six responses listed in the above table contain 1's and 0's and are for convenience in generating energy integrated fluxes for the specified energy ranges. The mid-point group energies (response 7 - 9) are the linear mid-point energies of the groups and can be utilized to obtain the average energy flux and energy leakage. Several miscellaneous functions (responses 10 and 23 - 33) were converted from the standard 51-group library used for the last several years at ORNL to analyze LMFBR shielding problems. The conversion was accomplished using the ROSIE program,[12] which employs a four-point quadratic fit interpolation scheme to convert between two arbitrary energy group structures. A flat energy weighting is implicit to the ROSIE interpolation.

The Bonner ball responses (11-19) were also generated using ROSIE. The original 100-group responses reported in Reference 6 were modified below 100 eV to correct for thermal upscatter effects.[13] This correction results in a reduction in the low-energy response for the smaller balls (3- and 4-in.) and an increase in the low-energy response for the larger balls (8-, 10-, and 12-in.).

Table 6. Response functions included in VELM61 and VELM22 libraries

Table Position[a]	Response
1	Total Neutron Flux
2	Neutron Flux E > 1.0 MeV
3	Neutron Flux E > 0.1 MeV
4	Neutron Flux 0.1 MeV > E > 2.38 eV
5	Neutron Flux E < 2.38 eV
6	Total Gamma-Ray Flux
7	Mid-Point Group Energies [eV] for Neutron and Gamma-Ray
8	Mid-Point Group Energies [eV] for Neutron Only
9	Mid-Point Group Energies [eV] for Gamma-Ray Only
10	Bare BF_3 Counter [counts/(n/cm^2)]
11	Cd-covered BF_3 Counter (2-in. B. Ball) [counts/(n/cm^2)]
12	Modified 3-in. Bonner Ball Response [counts/(n/cm^2)]
13	3.00-in. Bonner Ball Response [counts/(n/cm^2)]
14	4.03-in. Bonner Ball Response [counts/(n/cm^2)]
15	5.02-in. Bonner Ball Response [counts/(n/cm^2)]
16	6.00-in. Bonner Ball Response [counts/(n/cm^2)]
17	7.86-in. Bonner Ball Response [counts/(n/cm^2)]
18	9.86-in. Bonner Ball Response [counts/(n/cm^2)]
19	11.84-in. Bonner Ball Response [counts/(n/cm^2)]
20	Total ANSI Dose Response [(rem/hr)/(n/s.cm^2)]
21	Neutron ANSI Dose Response [(rem/hr)/(n/s.cm^2)]
22	Gamma-Ray ANSI Dose Response [(rem/hr)/(γ/s.cm^2)]
23	Hornyak Button > 120 keV [(ergs/g)/(n/cm^2)]
24	Hornyak Button > 270 keV [(ergs/g)/(n/cm^2)]
25	TLD Gamma-Ray Response - CaF_2 [(MeV/g)/(γ/cm^2)]
26	TLD Gamma-Ray Response - Li^7F [(MeV/g)/(γ/cm^2)]
27	TLD Neutron Sensitivity - CaF_2 [(MeV/g)/(n/cm^2)]
28	TLD Neutron Sensitivity - Li^7F [(MeV/gm)/(n/cm^2)]
29	Graphite Atom Displacement [barns]

Table 6. (Continued)

Table Position[a]	Response
30	SS-316 Atom Displacement [barns]
31	Iron Atom Displacement [barns]
32	Nominal 5% Uniform Elongation SS-316 593°C [1/(n/cm^2)]
33	Nominal 75°C NDTS A212B Steel [1/(n/cm^2)]
34	Iron Total Heating [W.s/cm]
35	Iron Neutron Heating [W.s/cm]
36	Iron Gamma-Ray Heating [W.s/cm]
37	SS-304 Total Heating [W.s/cm]
38	SS-304 Neutron Heating [W.s/cm]
39	SS-304 Gamma-Ray Heating [W.s/cm]
40	SS-316 Total Heating [W.s/cm]
41	SS-316 Neutron Heating [W.s/cm]
42	SS-316 Gamma-Ray Heating [W.s/cm]
43	Ordinary-Concrete Total Heating [W.s/cm]
44	Ordinary-Concrete Neutron Heating [W.s/cm]
45	Ordinary-Concrete Gamma-Ray Heating [W.s/cm]
46	B-10 (n,T2α) [barns]
47	B-11 Tritium Production [barns]
48	Na-23 (n,2n) [barns]
49	Na-23 (n,γ) [barns] Standard Weighting
50	Na-23 (n,γ) [barns] Flat Weighting
51	Na-23 (n,p) [barns]
52	Ar-40 (n,γ) [barns] Standard Weighting
53	Ar-40 (n,γ) [barns] Flat Weighting
54	Cr-50 (n,γ) [barns] Standard Weighting
55	Cr-50 (n,γ) [barns] Flat Weighting
56	Mn-55 (n,γ) [barns] Standard Weighting
57	Mn-55 (n,γ) [barns] Flat Weighting
58	Fe-54 (n,p) [barns]
59	Fe-58 (n,γ) [barns] Standard Weighting

Table 6. (Continued)

Table Position[a]	Response		
60	Fe-58 (n,γ)	[barns]	Flat Weighting
61	Co-59 (n,γ)	[barns]	Standard Weighting
62	Co-59 (n,γ)	[barns]	Flat Weighting
63	Ni-58 (n,p)	[barns]	
64	Ni-60 (n,p)	[barns]	
65	Mo-98 (n,γ)	[barns]	Standard Weighting
66	Mo-98 (n,γ)	[barns]	Flat Weighting
67	Ta-181 (n,γ)	[barns]	Standard Weighting
68	Ta-181 (n,γ)	[barns]	Flat Weighting

[a]For VELM61 (ID = 1000).

The ANSI dose responses[14] (20 - 22) were collapsed from the 171n/36γ Vitamin-C library[15] using the RIPOF program[12] with the Vitamin-C weighting function stripped off its fusion peak. The heating functions (responses 34 - 45) were collapsed from the MACKLIB-IV library[11] also using RIPOF as above. The B-11 tritium production cross section (response 47) was collapsed from the 174-group gas production file of the Vitamin-E library[10] using RIPOF with the standard weighting defined in Section II.4. The activation cross sections (responses 46, 48, 51, 58, 63, 64) were collapsed from the activation file of the Vitamin-E library also using RIPOF with the standard weighting. The (n,γ) activation cross sections (responses 49, 50, 52 - 57, 59 - 62, 65 - 68), derived from the Vitamin-E activation file, have double entries which are explained below.

In collapsing the dose factors, heating functions, and activation cross sections, both the standard weighting and the flat weighting have been considered. In all cases except the (n,γ) cross sections, the variation in each broad group due to the differences in weighting is small, generally less than 2%. In the case of the (n,γ) reaction, however, the cross section for the last broad group in the 61-neutron-group structure using the standard weighting is about 60% larger than that using the flat weighting. Since the (n,γ) cross section for the last group is always the largest of all groups, the 60% deviation in this group alone may significantly change the calculated activation rates. Therefore, the (n,γ) cross sections collapsed with both weightings are included in the libraries. It is suggested that the users consider both (n,γ) cross sections in their calculations. If the activation rates calculated from the two cross-section sets are significantly at odds, then some more scrutiny may be warranted to determine which set is more appropriate for the particular situation (location of the activated product in the reactor, for example). From the fine-group fluxes shown in Figs. 3-5 for the sodium-iron geometry, one can argue that the flat weighting is the more appropriate for collapsing the last two fine groups into the last broad group for the response functions in the VELM61 library.

IV. CONCLUSION

We have presented information intended to help users of the VELM61 and VELM22 libraries apply them intelligently. Though the libraries were specifically designed for sodium-cooled reactor shield analysis, part of the libraries is general enough for most other purposes until more appropriate problem-dependent cross-section libraries based on ENDF/B-V are available. For example, the cross sections generated using the standard and the $1/E\Sigma_t$ weighting functions are largely problem-independent. For sodium-cooled reactor shield studies, a thorough understanding of the present report is essential for making proper choices among the multiple entries of cross-section sets of a given material. We also recommend that the 22n/10γ library be used first for scoping calculations of a new problem, then the 61n/23γ library be applied for the final results. This should be easy to accomplish since cross-section sets in both libraries have the same contents and identifications.

V. ACKNOWLEDGEMENTS

The authors are grateful to W. W. Engle, Jr., R. W. Roussin, W. E. Ford III, J. E. White, C. O. Slater, and J. V. Pace III for advice during the course of this work. The authors are also eager to thank A. C. Alford for her pleasant cooperation in typing several extensive revisions of this report. This research is funded by the U.S. Department of Energy under contract with Martin Marietta Energy Systems, Inc.

REFERENCES

1. C. R. Weisbin, R. W. Roussin, J. J. Wagschal, J. E. White, and R. Q. Wright. "Vitamin-E: An ENDF/B-V Multigroup Cross Section Library for LMFBR Core and Shield, LWR Shield, Dosimetry and Fusion-Blanket Technology," Oak Ridge National Laboratory Report ORNL-5505 (ENDF-274), 1979. A recent release of Vitamin-E by the Radiation Shielding Information Center was dated August 20, 1985 and denoted DLC-113B.

2. W. W. Engle, Jr. "A User's Manual for ANISN, A One Dimensional Discrete Ordinates Transport Code with Anisotropic Scattering," Oak Ridge Gaseous Diffusion Plant Report K-1693 (1967), Updated Version (1973).

3. G. C. Haynes, "The AXMIX Program for Cross Section Mixing and Library Arrangement," Oak Ridge National Laboratory Technical Memorandum ORNL/TM-5295 (1974).

4. D. T. Ingersoll and C. O. Slater. "DOGS - A Collection of Graphics for Support of Discrete Ordinates Codes," Oak Ridge National Laboratory Technical Memorandum ORNL/TM-7188 (1980), Updated Version (1981).

5. N. M. Greene, W. E. Ford III, J. L. Lucius, J. E. White, L. M. Petrie, and R. Q. Wright. "AMPX: A Modular Code System for Generating Coupled Multigroup Neutron-Gamma Libraries from ENDF/B," Oak Ridge National Laboratory Technical Memorandum ORNL/TM-3706 (1976), Updated Version AMPX-II (1978).

6. R. E. Maerker, L. R. Williams, F. R. Mynatt, and N. M. Greene, "Response Functions for Bonner Ball Neutron Detectors," ORNL/TM-3451 (1971).

7. R. W. Roussin, "BUGLE-80: A Coupled 47-Neutron, 20-Gamma-Ray Group Library for LWR Shielding Calculations," DLC-75, RSIC Data Library Collection, Oak Ridge National Laboratory (1980).

8. A. de Carli and J. P. Trapp, "The Adjusted LMFBR Shielding Formulaire PROPANE Performance and Validation of Version 1 Experimental Program JASON for Version 2," Proceedings of the Sixth Int. Conf. on Radiation Shielding, May 16-20, 1983, Tokyo, Japan; CONF-830538 (1983).

9. D. T. Ingersoll. "TSF Na/Fe Experiment Used to Supply Potential Group Structures for LSPB Cross-Section Library," Presented at General Electric LSPB meeting (1983).

10. R. W. Roussin. Oak Ridge National Laboratory, private communication (1985).

11. Y. Gohar and M. A. Abdou, "A Library of Nuclear Response Functions Generated with the MACK-IV Computer Program from ENDF/B-IV," ANL/FPP/TM-106, Argonne National Laboratory (1978).

12. D. T. Ingersoll, Oak Ridge National Laboratory, Private Communication (1986).

13. R. E. Maerker, F. J. Muckenthaler, R. C. Childs, and M. L. Gritzner, "Final Report on a Benchmark Experiment for Neutron Transport in Thick Sodium," Oak Ridge National Laboratory Report ORNL-4880 (1974).

14. M. E. Battat, "American National Standard Neutron and Gamma-ray Flux-to-Dose-Rate Factors," ANSI/ANS-6.1.1, American Nuclear Society (1977).

15. R. W. Roussin, C. R. Weisbin, J. E. White. N. M. Greene, R. Q. Wright, and J. B. Wright, "Vitamin-C: The CTR Processed Multigroup Cross Section Library for Neutronics Studies," ORNL/RSIC-37, Oak Ridge National Laboratory (1980).

ORNL/TM-10302
Distribution Category
UC-79-d

INTERNAL DISTRIBUTION

1. R. G. Alsmiller
2. B. L. Broadhead
3. J. A. Bucholz
4-8. D. G. Cacuci
9. R. L. Childs
10. S. N. Cramer
11. J. D. Drischler
12. M. B. Emmett
13. W. W. Engle, Jr.
14. W. E. Ford
15-19. C. Y. Fu
20. T. A. Gabriel
21. N. M. Greene
22-26. D. T. Ingersoll
27. J. O. Johnson
28. J. E. Jones, Jr.
29. R. A. Lillie
30. R. E. Maerker
31. F. C. Maienschein
32. B. F. Maskewitz
33. F. J. Muckenthaler
34. F. R. Mynatt
35. J. V. Pace, III
36. C. V. Parks
37. R. W. Peelle
38. R. T. Primm
39. W. A. Rhoades
40. B. D. Rooney
41. R. W. Roussin
42. R. T. Santoro
43. C. O. Slater
44. J. S. Tang
45. R. C. Ward
46. C. R. Weisbin
47. R. M. Westfall
48. L. R. Williams
49. J. E. White
50. A. Zucker
51. P. W. Dickson, Jr. (Consultant)
52. G. H. Golub (Consultant)
53. R. M. Haralick (Consultant)
54. D. Steiner (Consultant)
55-56. Central Research Library
57. Y-12 Technical Library Document Reference Section
58-59. Laboratory Records Department
60. Laboratory Records ORNL, RC
61. ORNL Patent Office
62-64. Engineering Physics Information Center
65. EPMD Reports Office

EXTERNAL DISTRIBUTION

66. Office of the Assistant Manager for Energy Research and Development, Oak Ridge Operations, Department of Energy, P.O. Box E, Oak Ridge TN 37830.

67. J. E. Brunings, Program Manager, SAFR, Rocketdyne Division, Rockwell International Corp., 6633 Canoga Avenue, Canoga Park CA 91304.

68. W. L. Bunch, Westinghouse-Hanford, 400 Area Trailer 1, Richland WA 99352.

69. R. K. Disney, Westinghouse Electric Company, P.O. Box 158, Madison PA 15663.

70. A. R. Gilchrist, Manager, Prism Technology Program, Nuclear Systems Technology Operation, General Electric Co., P.O. Box 3508, Sunnyvale CA 94088.

71. W. H. Harless, General Electric Company, P.O. Box 3508, Sunnyvale CA 94088.

72. P. B. Hemmig, Advanced Technology Development, Office of Technology Support Programs, U.S. Department of Energy, Washington DC 20545.

73. R. J. Neuhold, Director, Advanced Technology Development, U.S. Department of Energy, Washington DC 20545.

74. E. R. Specht, Rockwell International, 6633 Canoga Avenue, Canoga Park CA 91304.

75-175. Given distribution as shown in TID-4500, LMFBR - Physics Base Technologies UC-79-d.